Supporting Information

Steric and Electronic Control of an Ultrafast Isomerizaiton.

Tyler M. Porter, Andrew L. Ostericher, and Clifford P. Kubiak*.

Department of Chemistry and Biochemistry, University of California San Diego, 9500 Gilman Drive, La Jolla, California 92093-0358, United States.

Table of Figures

Table of Tables

Experimental.

Preparation and Purification: The 2,3-hexafluorobutyne was used as received from Oakwood Chemicals, the triruthenium doedecacarbonyl was used as received from Acros Organics, and the methyldiphenylphosphine was used as received from Alfa aesar. The cyclohexane stabilized dichloromethane (DCM), was purchased from VWR International LLC, deoxygenated and dried over alumina columns on a custom built solvent system under an argon atmosphere and stored over activated 4 Å molecular sieves in a nitrogen filled glove box. The 2,3-dithiolene and $Ru(S_2C_2(CF_3)_2)(CO)(L)_2$ were prepared following modified literature reported procedures.[1-2]

$Ru(S_2C_2(CF_3)_2)(CO)(L)_2$ (2–8): Under an inert atmosphere a 100 mL Schlenk flask was charged with 200 mg (0.32 mmol, 1 eq.) triruthenium dodecacarbonyl, 325 mg (1.44 mmol, 4.5 eq) of bis(perfluoromethyl)-1,2-dithietene, and approximately 40 mL of *n*-heptane. After refluxing for one hour, a stoichiometeric amount of the phosphine ligand (L = $P((p\text{-Me})Ph)_3$: 187 mg (**2**), $P((p\text{-Cl})Ph)_3$: 231.1 mg (**3**), $P(Ph)_2Me$: 179.6 mg (**4**), $P(Ph)_2Et$: 186.3 mg (**5**), $P(Ph)_2{}^{i}Pr$: 109.2 mg (**6**), $P(Ph)_2{}^{t}Bu$: 218.1 mg (**7**), $P(CH_2Ph)_3$: 223.2 mg (**8**)) was added under a nitrogen stream followed by an additional 12 hour reflux. The solvent was then removed under vaccum to yield an orange/red solid and the ruthenium complexes were isolated by column chromatography. Using 7:3 Hexanes:DCM as the elutant, the complexes were isolated as the second red band (green for **7**) using an elutant of 7:3 Hexanes:DCM.

$Ru(S_2C_2(CF_3)_2)(CO)P((p\text{-Me})Ph)_3$ (**2**). The complex, $Ru(S_2C_2(CF_3)_2)(CO)(P((p\text{-Me})Ph)_3)_2$, was recrystallized at –30 °C by layering a saturated DCM solution with pentane, affording bright yellow/orange crystals identified as the axial iosomer (**2c**) of $Ru(S_2C_2(CF_3)_2)(CO)(P((p\text{-Me})Ph)_3)_2$. Yield: 187.0 mg (62%). ^{1}H NMR (DCM-d_2, 500 MHz): δ (ppm) = 6.97 (m, 12H, C*H*), 6.90 (m, 12H, C*H*), 2.31 (s, 18H, CH_3). ^{13}C {^{1}H} NMR (DCM-d_2, 500 MHz): δ (ppm) = 230.6 (t, *C*O, J = 5 Hz), 144.89 (m, S*CC*S), 140.94 (s, *C*CH_3), 134.1 (t, *C*H, J = 5 Hz), 130.8 (m, P*C*), 129.04 (t, *C*H, *J* = 4 Hz), 123.2 (q, *C*F_3, J = 276 Hz), 21.36 (s, *C*H_3). ^{19}F NMR (DCM-d_2, 500 MHz): δ (ppm) = -53.94. 31P NMR (DCM-d_2, 500 MHz): δ (ppm) = 46.91. Anal. Calc for $C_{47}H_{42}F_6OS_2P_2Ru$: C, 58.56 %; H, 4.39 %; S, 6.65%; Found: C, 58.80 %; H, 4.24%; S, 6.19%; FTIR (CH_2Cl_2, cm^{-1}): 1944 cm^{-1} (br). UV-Vis (nm) 389, 465, 554.

$Ru(S_2C_2(CF_3)_2)(CO)P((p\text{-Cl})Ph)_3$ (**3**). The complex, $Ru(S_2C_2(CF_3)_2)(CO)(P((p\text{-Cl})Ph)_3)_2$, was recrystallized at –30 °C by layering a saturated DCM solution with pentane, affording bright yellow/orange crystals identified as the axial iosomer (**3c**) of $Ru(S_2C_2(CF_3)_2)(CO)(P((p\text{-Cl})Ph)_3)_2$. Yield: 231.1 mg (68%). ^{1}H NMR (DCM-d_2, 500 MHz): δ (ppm) = 7.24 (dd, 12H, C*H*, J = 8.6, 1.5 Hz), 6.94 (m, 12H, C*H*). ^{13}C {^{1}H} NMR (DCM-d_2, 500 MHz): δ (ppm) = 202.11 (t, *C*O, J = 15 Hz), 146.48 (m, S*CC*S), 137.9 (s, *C*Cl), 135.2 (t, *C*H, J = 15 Hz), 131.5 (P*C*, m), 130.7 (*C*Cl), 129.1 (t, *C*H, J = 5 Hz), 122.7 (q, *C*F_3, J = 276 Hz). ^{19}F NMR (DCM-d_2, 500 MHz): δ (ppm) = -54.25. ^{31}P NMR (DCM-d_2, 500 MHz): δ (ppm) = 49.14. Anal. Calc for $C_{41}H_{24}F_6Cl_6OS_2P_2Ru$: C, 45.33 %; H, 2.23 %; S, 5.90 %; Found: C, 45.23 %; H, 2.36 %; S, 6.21%; FTIR (CH_2Cl_2, cm^{-1}): 1963 (br). UV-Vis (nm) 389, 473, 554.

$Ru(S_2C_2(CF_3)_2)(CO)(PPh_2(Me))_2$ (4). The complex, $Ru(S_2C_2(CF_3)_2)(CO)(PPh_2(Me))_2$, was recrystallized at –30 °C by layering a saturated DCM solution with pentane,

affording bright yellow/orange crystals identified as the axial iosomer (**4c**) of $Ru(S_2C_2(CF_3)_2)(CO)(PPh_2Me)_2$. Yield: 179.6 mg (76%). ^{1}H NMR (DCM-d_2, 500 MHz): δ (ppm) = 7.38 (m, 4H, C*H*), 7.28 (m, 8H, C*H*), 7.11 (m, 8H, C*H*), 1.75 (d, 6H, PCH_3, J = 9 Hz). ^{13}C {^{1}H} NMR (DCM-d_2, 500 MHz): δ (ppm) = 201.57 (t, *C*O, J = 15 Hz), 144.62 (m, S*CC*S), 135.7 (m, P*C*), 132.2 (dt, *C*H, J = 118, 5 Hz), 130.8 (d, *C*H, J = 41 Hz), 128.8 (dt, *C*H, J = 27, 6 Hz), 123.22 (q, *C*F_3, 276 Hz), 17.68 (dt, *C*H_3, J = 34, 12 Hz). ^{19}F NMR (DCM-d_2, 500 MHz): δ (ppm) = -52.87 (C*F*$_3$). ^{31}P NMR (DCM-d_2, 500 MHz): δ (ppm) = 33.95 (*P*Ph_2Me). Anal. Calc for $C_{31}H_{26}F_6OS_2P_2Ru$: C, 49.27 %; H, 3.47 %; S, 8.49 %; Found: C, 49.42 %; H, 3.43 %; S, 8.33 %; FTIR (CH_2Cl_2, cm^{-1}): 1969 (s), 1940 (s). UV-Vis (nm) 370, 450, 522.

$Ru(S_2C_2(CF_3)_2)(CO)(PPh_2(Et))_2$ (**5**). The complex, $Ru(S_2C_2(CF_3)_2)(CO)(PPh_2(Et))_2$, was recrystallized at –30 °C by layering a saturated DCM solution with pentane, affording bright orange crystals identified as the axial iosomer (**5c**) of $Ru(S_2C_2(CF_3)_2)(CO)(PPh_2Me)_2$. Yield: 186.3 mg (76%). ^{1}H NMR (DCM-d_2, 500 MHz): δ (ppm) = 7.41 (dt, 4H, C*H*, J = 31.3, 7.2 Hz), 7.30 (dt, 8H, C*H*, J = 22.4, 7.2 Hz), 7.07 (dt, 8H, C*H*, J = 63, 8.1 Hz), 2.11 (dseptet, 4H, CH_2, J = 74.3, 7.3 Hz), 0.63 (dt, 6H, CH_3, J = 16.9, 7.3 Hz). ^{13}C {^{1}H} NMR (DCM-d_2, 500 MHz): δ (ppm) = 201.5 (t, CO, J = 14 Hz), 144.1 (m, S*CC*S), 133.5 (m, P*C*), 133.0 (m, *C*H), 130.6 (d, *C*H, J = 8 Hz), 128.6 (dt, *C*H, J = 15, 5 Hz), 123.3 (q, *C*F_3, J = 276 Hz), 24.7 (m, *C*H_2), 9.0 (s, *C*H_3). ^{19}F NMR (DCM-d_2, 500 MHz): δ (ppm) = –52.7 (C*F*$_3$). ^{31}P NMR (DCM-d_2, 500 MHz): δ (ppm) = 46.20 (*P*Ph_2Me). Anal. Calc for $C_{33}H_{30}F_6OS_2P_2Ru$: C, 50.57 %; H, 3.86 %; S, 8.18 %; Found: C, 50.92 %; H, 4.29 %; S, 7.81 %; FTIR (CH_2Cl_2, cm^{-1}): 1970 (s), 1933 (s). UV-Vis (nm) 370, 454, 530.

$Ru(S_2C_2(CF_3)_2)(CO)(PPh_2(^iPr))_2$ (**6**). The complex, $Ru(S_2C_2(CF_3)_2)(CO)(PPh_2(^iPr))_2$, was recrystallized at –30 °C by from acetonitrile, affording bright yellow/orange crystals identified as the axial iosomer (**6c**) of $Ru(S_2C_2(CF_3)_2)(CO)(PPh_2(t\text{-}Bu))_2$. The coordinated acetonitrile can be removed under vacuum, where crystals are observed to transition from yellow/orange to a deep red. Yield: 109.2 mg (43%). ^{1}H NMR (DCM-d_2, 500 MHz): δ (ppm) = 7.38 (dt, 4H, C*H*, J = 39.1, 7.5 Hz), 7.29 (dt, 8H, C*H*, J = 17.2, 8.5 Hz), 7.04 (dt, 8H, C*H*, J = 116, 8.6 Hz), 2.60 (m, 2H, C*H*$(CH_3)_2$), 0.72 (ddd, 12H, CH(C$H_3)_2$, J = 109, 16.2, 6.8 Hz). ^{13}C {^{1}H} NMR (DCM-d_2, 500 MHz): δ (ppm) = 203.7 (t, *C*O, J = 14 Hz), 143.2 (m, S*CCS*), 133.9 (dt, *C*H, J = 51, 4 Hz) 131.4 (m, P*C*), 130.1 (d, *C*H, J = 54 Hz), 127.9 (dt, *C*H, J = 34, 5 Hz), 122.9 (q, *C*F_3, J = 276 Hz), 31.7 (dt, *C*H$(CH_3)_2$, J = 28.7, 7.2 Hz), 18.3 (d, CH(*C*$H_3)_2$, J = 27.4 Hz). ^{19}F NMR (DCM-d_2, 500 MHz): δ (ppm) = -52.86. ^{31}P NMR (DCM-d_2, 500 MHz): δ (ppm) = 57.07. Anal. Calc for $C_{35}H_{34}F_6OS_2P_2Ru$•ACN: C, 52.11 %; H, 4.37 %; N, 1.64 %; S, 7.52 %; Found: C, 51.86 %; H, 4.54 %; N, 2.23 %; S, 7.55 %; FTIR (cm^{-1}): 1942 (br). UV-Vis (nm) 386, 455, 554.

$Ru(S_2C_2(CF_3)_2)(CO)(PPh_2(^tBu))_2$ (**7**). The complex, $Ru(S_2C_2(CF_3)_2)(CO)(PPh_2(^tBu))_2$, was recrystallized at –30 °C by layering a saturated DCM solution with pentane, affording dark red/violet crystals identified as the equatorial iosomer (**7a**) of $Ru(S_2C_2(CF_3)_2)(CO)(PPh_2(t\text{-}Bu))_2$. Yield: 218.1 mg (83%). ^{1}H NMR (DCM-d_2, 500 MHz): δ (ppm) = 7.35 (m, 6H, C*H*), 7.28 (m, 2H, C*H*), 7.11 (m, 12H, C*H*), 0.76 (d, 18H, CH_3, J = 15 Hz). ^{13}C {^{1}H} NMR (DCM-d_2, 500 MHz): δ (ppm) = 202.26 (t, *C*O, 15 Hz), 144.77 (m, S*CC*S), 134.3 (d, CH, J = 217 Hz), 132.7 (dd, P*C*, J = 275 Hz), 129.8 (d, *C*H, J = 55

Hz), 127.35 (d, *C*H, J = 65 Hz), 123.06 (q, *C*F_3, J = 275 Hz), 36.1 (*C*$(CH_3)_3$, m), 28.15 (s, C(*C*$H_3)_3$). ^{19}F NMR (DCM-d_2, 500 MHz): δ (ppm) = -53.44. ^{31}P NMR (DCM-d_2, 500 MHz): δ (ppm) = 74.47. Anal. Calc for $C_{37}H_{38}F_6OS_2P_2Ru$: C, 52.92 %; H, 4.56 %; S, 7.63 %; Found: C, 53.32 %; H, 4.53 %; S, 7.84 %; FTIR (CH_2Cl_2, cm^{-1}): 1956 (br). UV-Vis (nm) 377, 468, 594.

Ru($S_2C_2(CF_3)_2$)(CO)($P(CH_2Ph)_3$)$_2$ (**8**). The complex, Ru($S_2C_2(CF_3)_2$)(CO)($P(CH_2Ph)_3$)$_2$, was recrystallized at –30 °C by layering a saturated DCM solution with pentane, affording dark red/violet crystals identified as the axial iosomer (**8a**) of Ru($S_2C_2(CF_3)_2$)(CO)($P(CH_2Ph)_3$)$_2$. Yield: 223.2 mg (74%). ^{1}H NMR (DCM-d_2, 500 MHz): δ (ppm) = 7.24 (m, 18H, C*H*), 6.92 (m, 12H, C*H*), 3.07 (m, 12H, CH_2). ^{13}C {^{1}H} NMR (DCM-d_2, 500 MHz): δ (ppm) = 199.78 (t, *C*O, J = 15 Hz), 143.12 (m, S*CC*S), 133.9 (P*C*), 130.71 (*C*H), 129.19 (*C*H), 127.56 (*C*H), 123.38 (q, CF_3, J = 272 Hz), 38.28 (m, *C*H_2). ^{19}F NMR (DCM-d_2, 500 MHz): δ (ppm) = -53.32. ^{31}P NMR (DCM-d_2, 500 MHz): δ (ppm) = 51.07. Anal. Calc for $C_{47}H_{42}F_6OS_2P_2Ru$: C, 58.56 %; H, 4.39 %; S, 6.65 %; Found: C, 58.35 %; H, 4.72 %; S, 6.36 %; FTIR (CH_2Cl_2, cm^{-1}): 1966 (br). UV-Vis (nm) 525, 448, 367.

Ru($S_2C_2(CF_3)_2$)(CO)($P(Ph)_2(Me)$)$_3$ (**9**). The complex, Ru($S_2C_2(CF_3)_2$)(CO)($P(Ph)_2(Me)$)$_3$, was synthesized by dissolution of 100.0 mgs (0.132 mmol) of complex **4** into DCM, followed by the addition of 29.1 mg (0.146 mmol) of diphenylmethylphosphine. The complex was recrystallized at –30 °C by layering a saturated DCM solution with pentane, affording bright yellow crystals identified as the trisphosphine adduct Ru($S_2C_2(CF_3)_2$)(CO)($P(Ph)_2(Me)$)$_3$ (**9**). Yield: 103.7 mg (82 %). ^{1}H NMR (DCM-d_2, 500 MHz): δ (ppm) =7.35 (s, 12H, C*H*), 7.25 (s, 6H, C*H*), 7.15 (s, 12H, C*H*), 1.82 (s, 9H, PCH_3,). ^{13}C {^{1}H} NMR (DCM-d_2, 500 MHz): δ (ppm) = 202.76 (s, *C*O), 150.24 (m, S*CC*S) 136.09 (s, P*C*), 132.12 (s, *C*H), 129.37 (s, *C*H), 128.23 (*C*H), 123.05 (q, *C*F_3, J = 272 Hz), 11.61 (s, P*C*H_3). ^{19}F NMR (DCM-d_2, 500 MHz): δ (ppm) = –54.61. ^{31}P NMR (DCM-d_2, 500 MHz): δ (ppm) = 8.95, –6.15; Anal. Calc for $C_{44}H_{39}F_6OS_2P_3Ru$: C, 55.29 %; H, 4.11 %; S, 6.71 %; Found: C, 55.39 %; H, 4.11 %; S, 7.13 %; FTIR (CH_2Cl_2, cm^{-1}): 1948 (s). UV-Vis (nm) 343, 457.

Infrared Data Collection and Analysis. Infrared spectra were collected on a Bruker Equinox 55 FTIR spectrometer using a SPECAC flow through optical cryostat (model, 21525) with a 1.12 mm path length (determined from infringing pattern), CaF_2 windowed cell enclosed in a vacuum jacketed housing. Solutions were prepared in a nitrogen filled glove box using pre-dried DCM and *pure* orange crystals. Cell temperature (± 1 °C) was regulated by addition of liquid nitrogen/methanol to the cooling compartment while heating the cell compartment to the desired temperature with a computer controlled thermocouple/heating coil system. Both solutions of the complex and solvent blanks were recorded at temperatures ranging from 30 °C to –68 °C to ensure accurate solvent subtraction. To obtain the integrated spectral areas for the exchanging species, spectral curve fitting was carried out in IGOR Pro (WaveMetrics Inc., version 7.05).

Density Functional Theory Analysis. Calculations were performed in the ORCA software suite (version 3.0.3) at the BP86 level of theory with the RIJCOSX approximation.[3-7] Ruthenium, phosphorous, sulfur, and oxygen atoms were treated with the DEF2-TZVP basis sets while DEF2-SVP was used for all other atoms.[8-16] Dispersion

corrections were applied using the atom-pairwise dispersion correction with a Becke-Johnson damping scheme (D3BJ), relativistic effects with the ZORA model, and solvation was accounted for using the COSMO solvation model in methylene chloride.[17-19] Analytical frequency calculations were performed at the same level of theory. Molecular graphics were constructed with the UCSF Chimera package.[20]

NMR Data Collection and Analysis. NMR spectra were recorded on a JEOL 500 MHz NMR spectrometer and analyzed using iNMR software. Samples were prepared in dichloromethane-d_2 and referenced to solvent residuals for ^{1}H and ^{13}C, trifluoroethanol for ^{19}F, and phosphoric acid for ^{31}P NMR. A total of 16 scans of 32768 data points from –2 to 14 ppm were collected for ^{1}H NMR, 16 scans of 65536 data points from –220 to 20 ppm for ^{19}F NMR, and 64 scans of 32768 data points from –250 to 150 ppm for ^{31}P NMR.

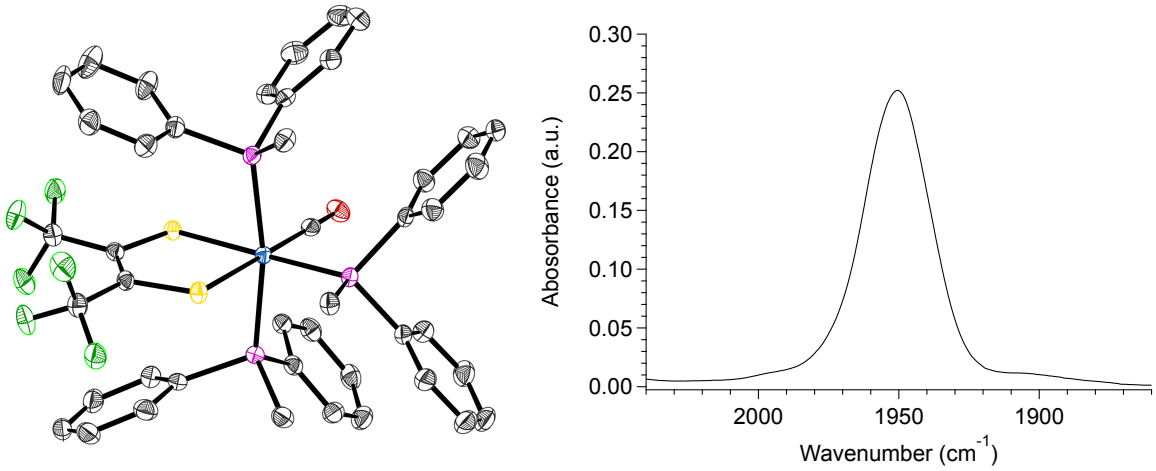

Figure S1. (left) ORTEP structure of $Ru((CF_3)_2C_2S_2)(CO)(P(Ph)_2(Me))_3$ (9) at 50% probability ellipsoids with hydrogen atoms omitted for clarity. (right) FTIR of 9 in DCM at 20 °C highlighting the narrow, single Gaussian ν(CO) band.

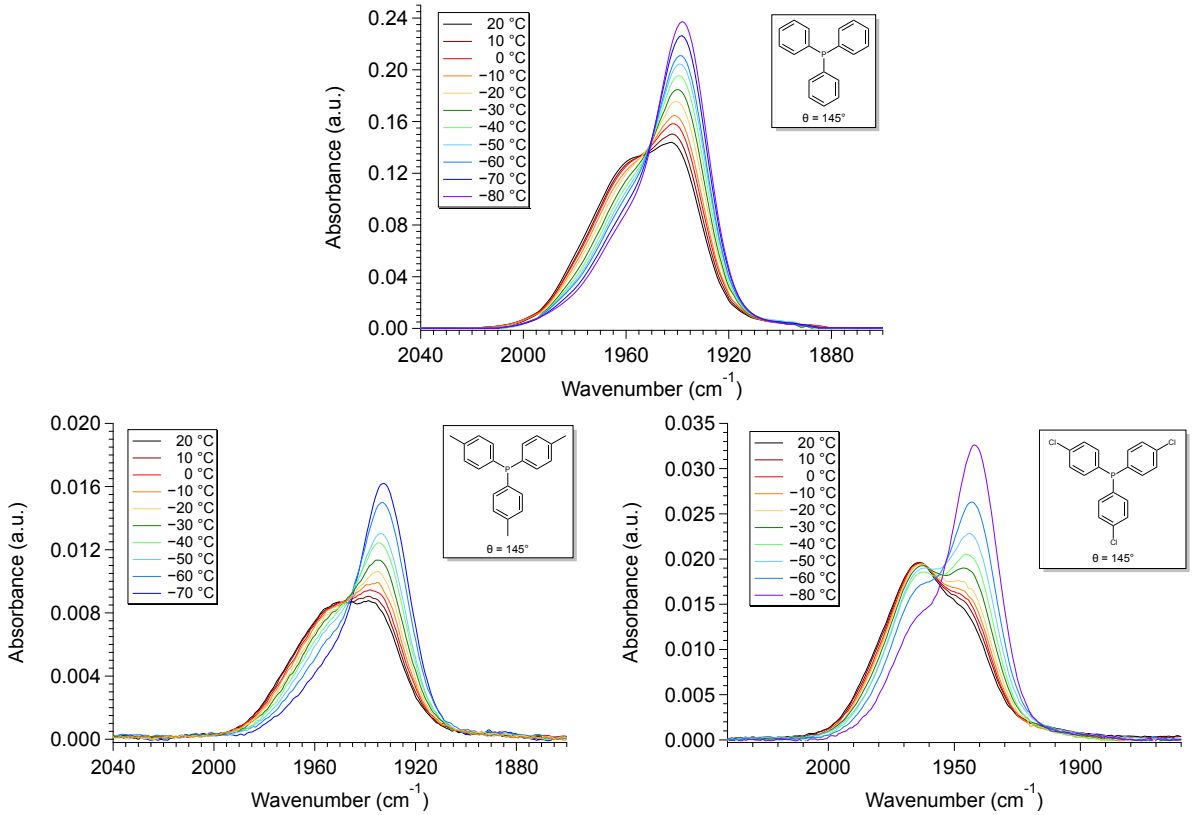

Figure S2. Variable temperature infrared (VT-FTIR) spectra for complexes **1** (top), **2**, (bottom left) and **3** (bottom right) in DCM from 20 °C to –70 °C.

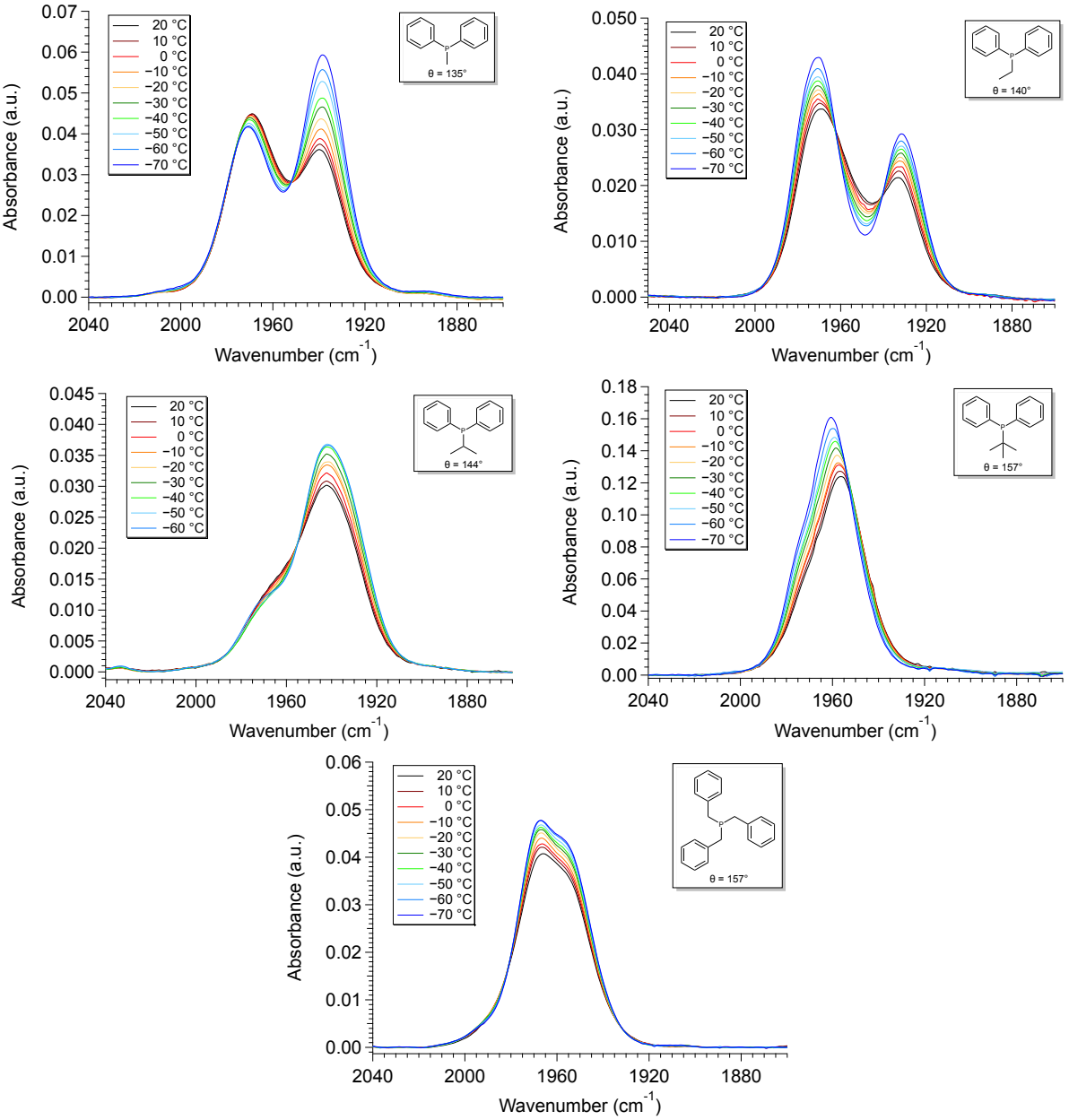

Figure S3. Variable temperature infrared (VT-FTIR) spectra for complexes **4**–**8** in DCM from 20 °C to –70 °C.

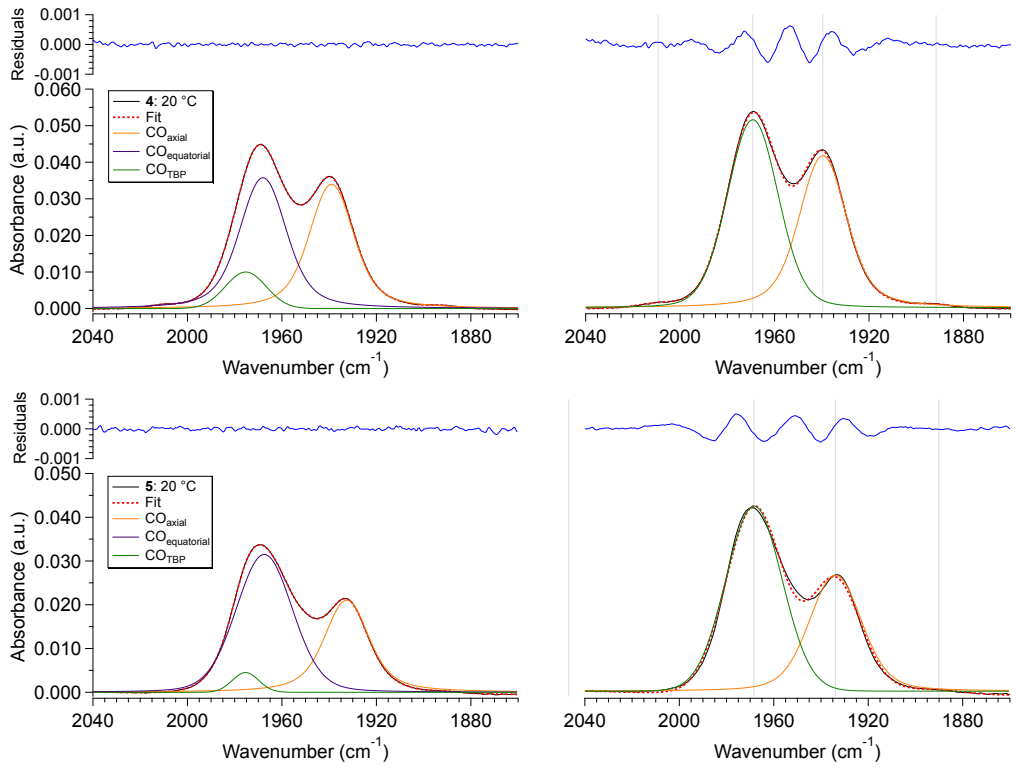

Figure S4. Three-component (left) and two-component (right) spectral deconvolution for complex **4** (top) and **5** (bottom).

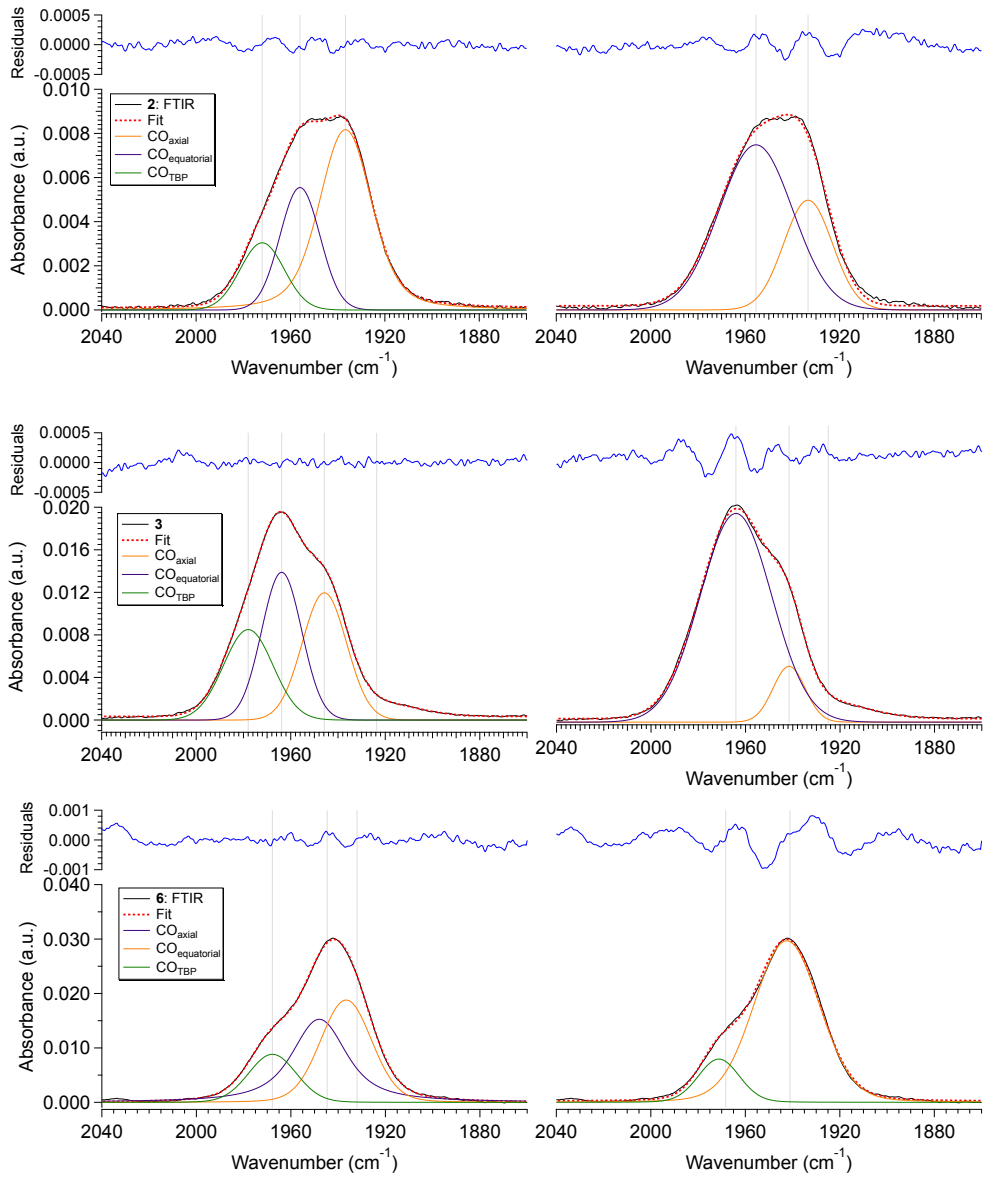

Figure S5. Three-component (left) and two-component (right) spectral deconvolution for complex **2** (top), **3** (middle), and **6** (top).

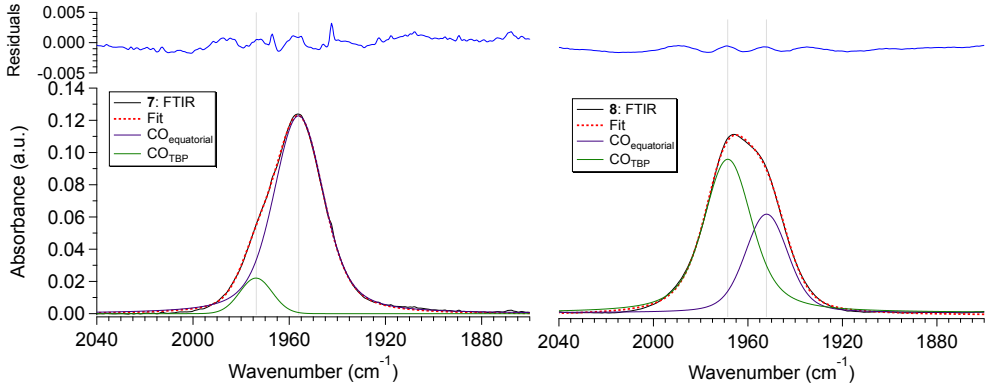

Figure S6. Two-component spectral deconvolution for complex **7** (left) and **8** (right).

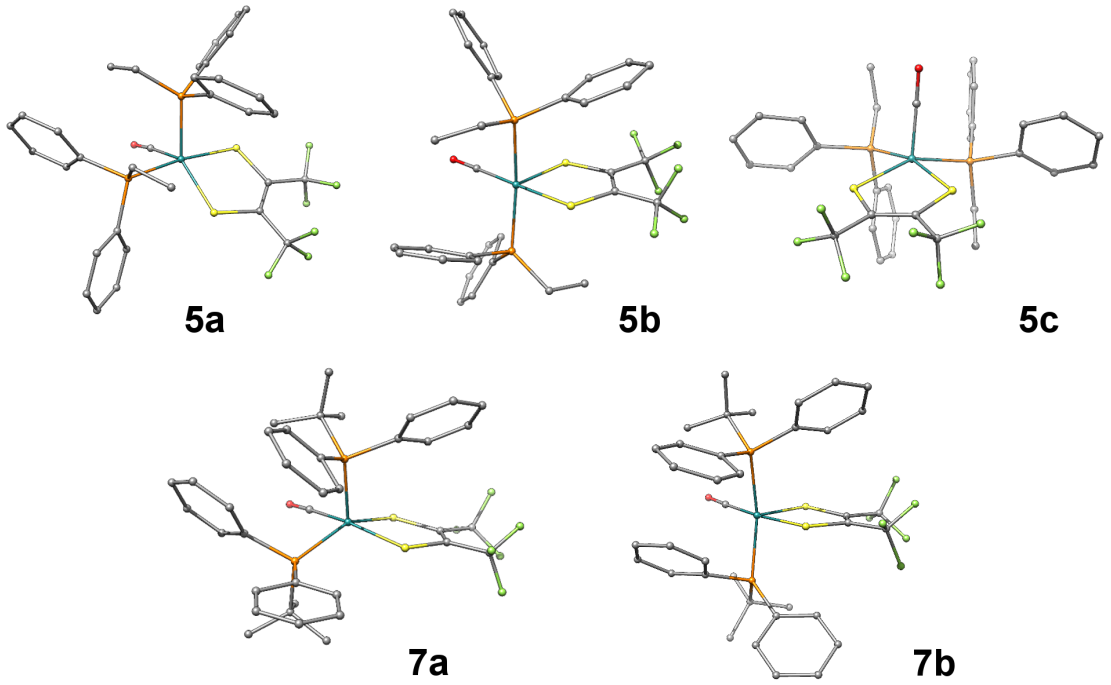

Figure S7. DFT optimized structures for complex **5** and **7**. All three isomers were found to be stable structures for **5** while only the $CO_{equatorial}$ and CO_{TBP} were observed to converge for **7**.

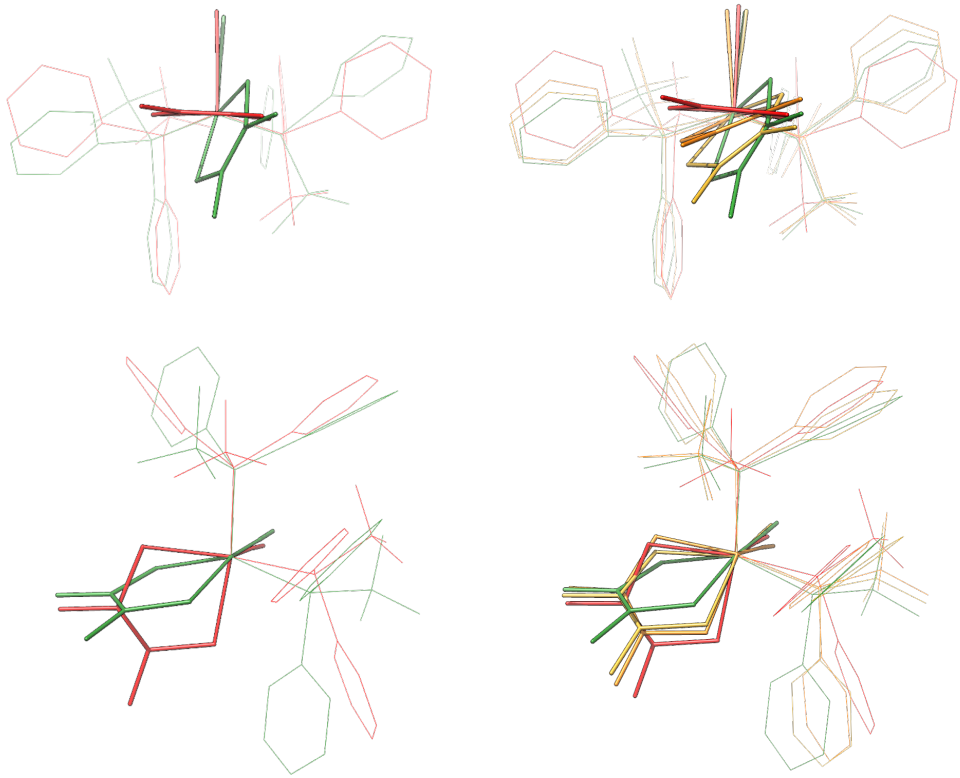

Figure S8. DFT optimization trajectory for isomer **7c** illustrating the transition from the starting coordinates of the CO_{axial} (red) isomer to the ending coordinates of the $CO_{equatorial}$ (green) isomer.

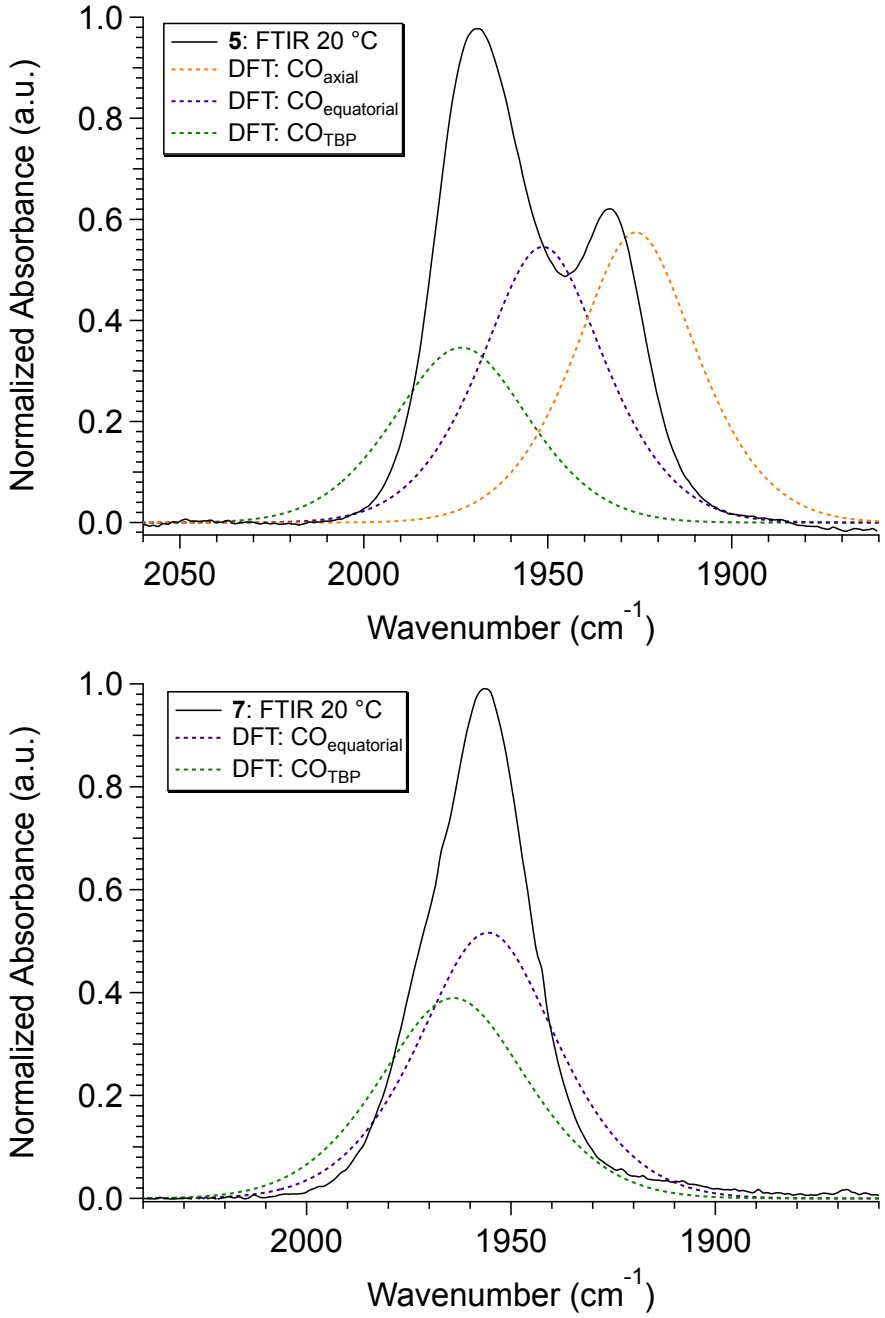

Figure S9. Comparison of DFT predicted FTIR (dashed) with the experimental (black, solid) FTIR for complexes **5** (top) and **7** (bottom).

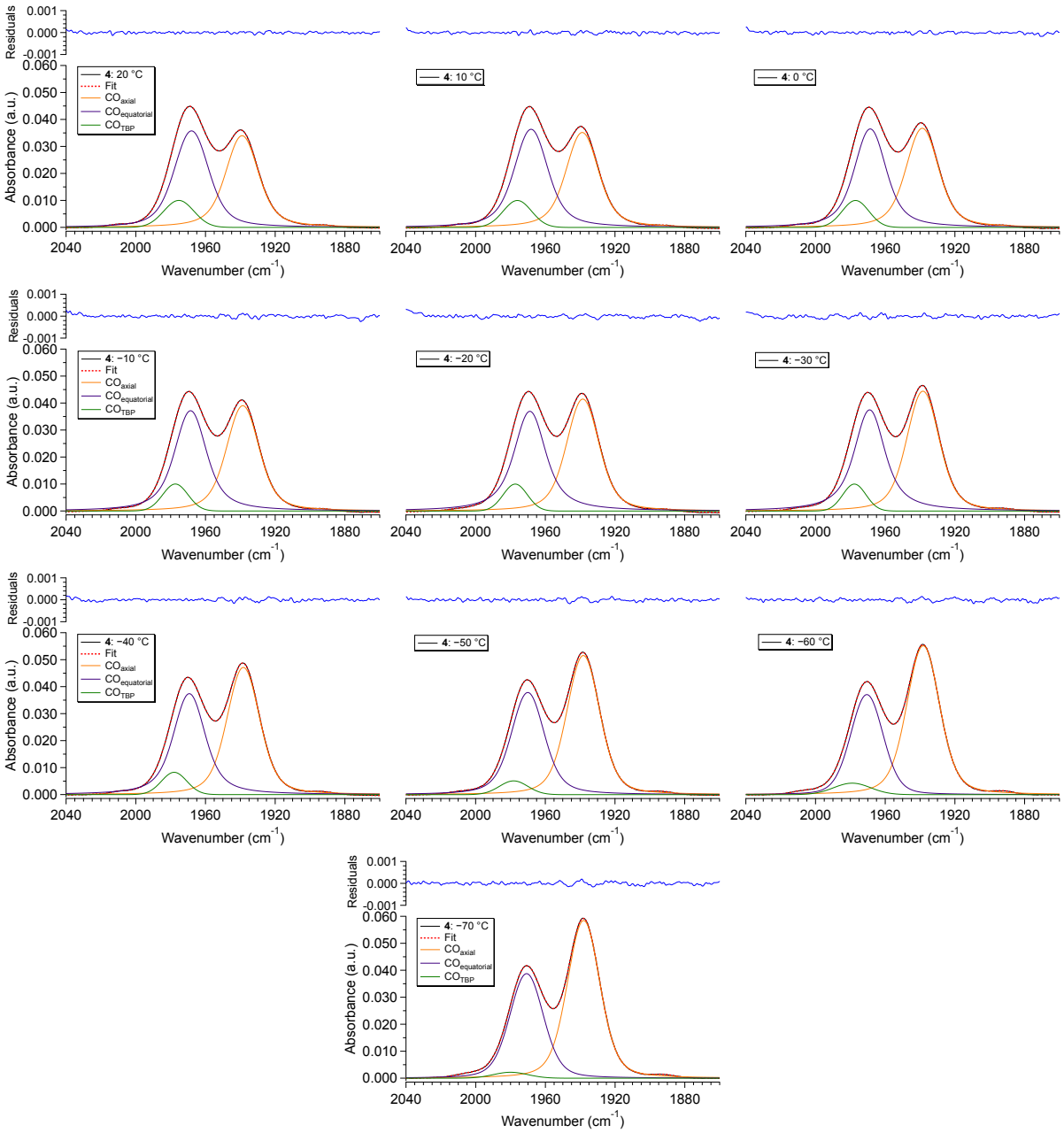

Figure S10. Spectral deconvolution of the variable temperature FTIR (VT-FTIR) spectra for complex **4**.

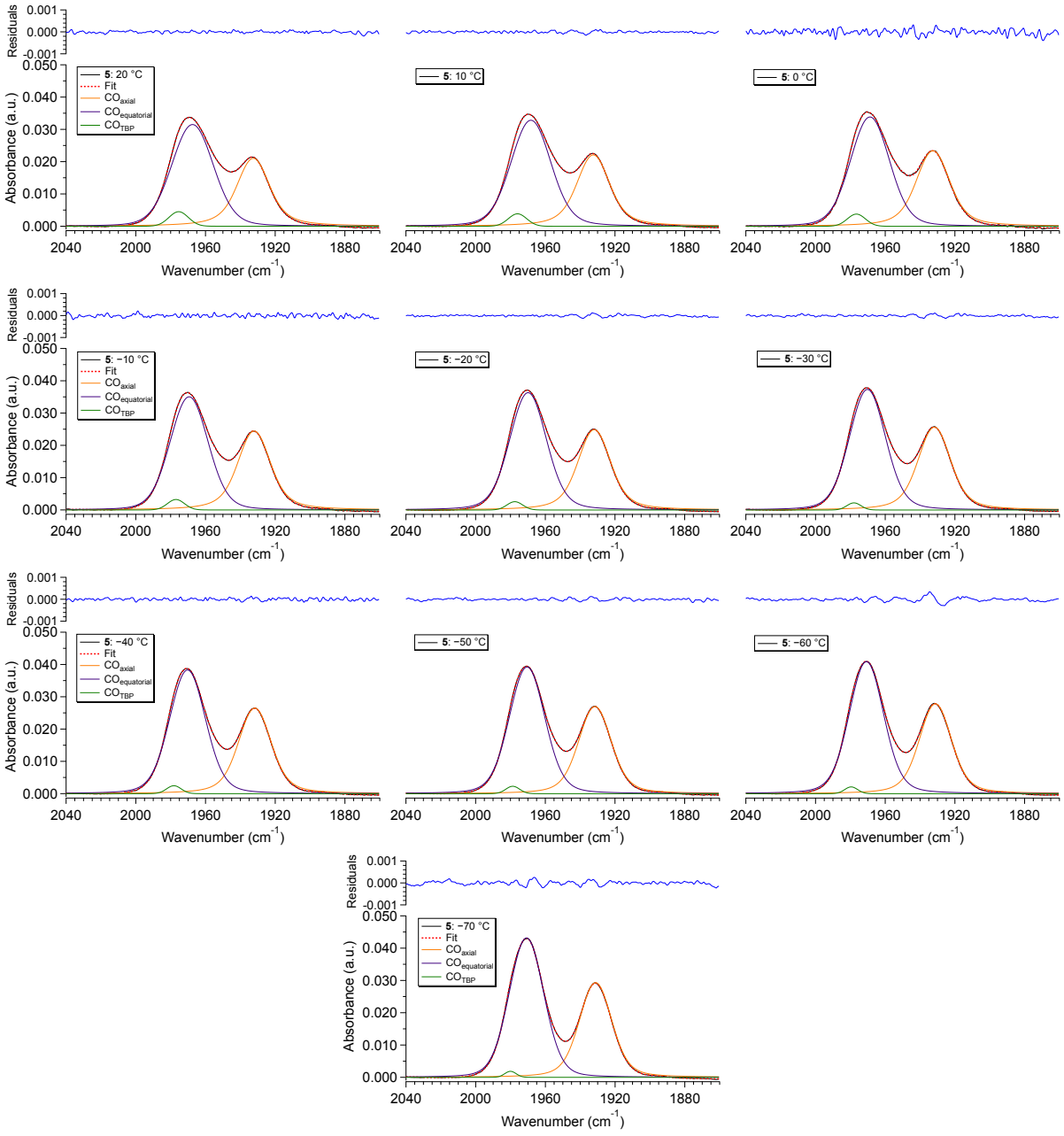

Figure S11. Spectral deconvolution of the VT-FTIR spectra for complex **5**.

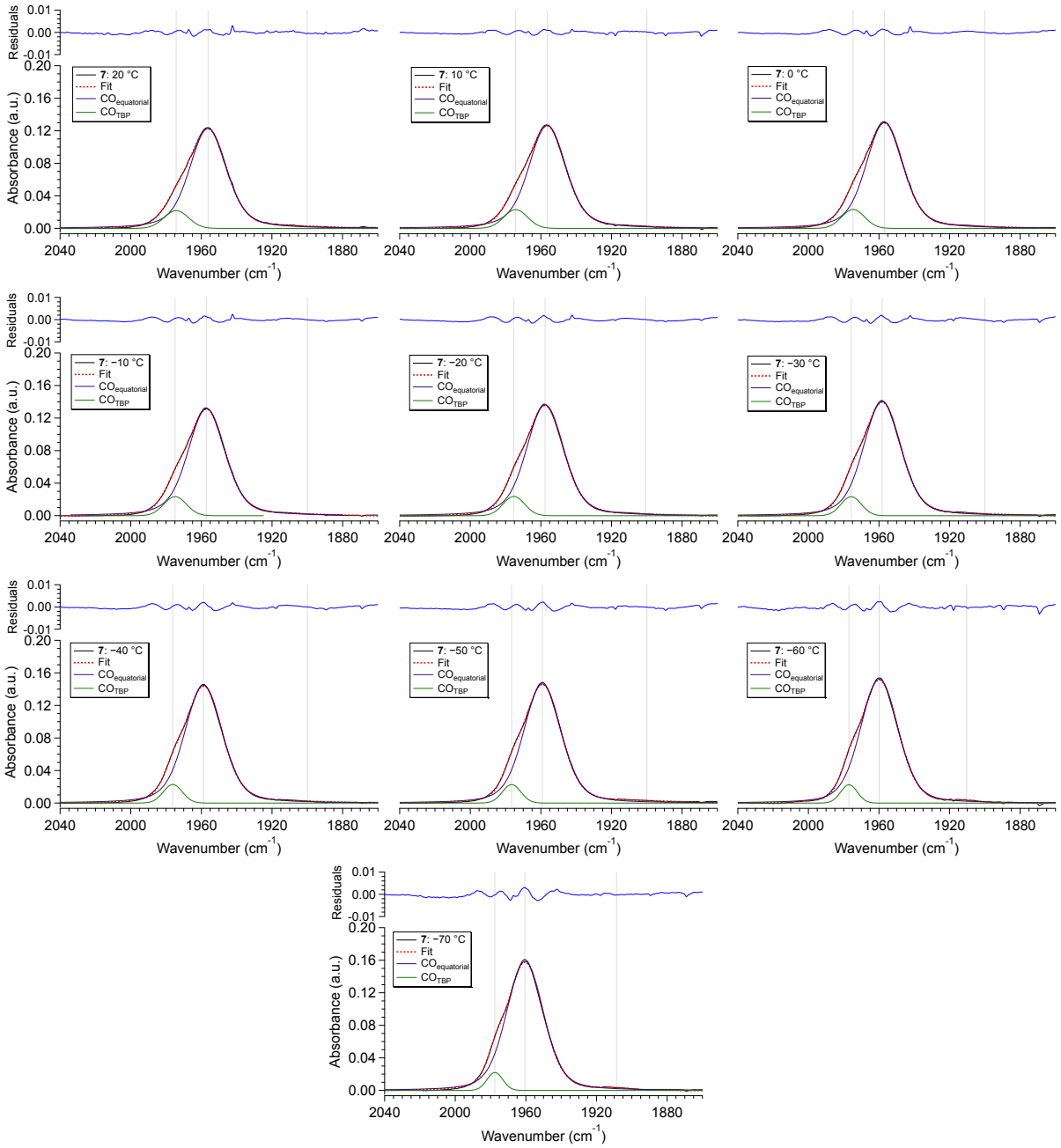

Figure S12. Spectral deconvolution of the variable temperature FTIR (VT-FTIR) spectra for complex **7**.

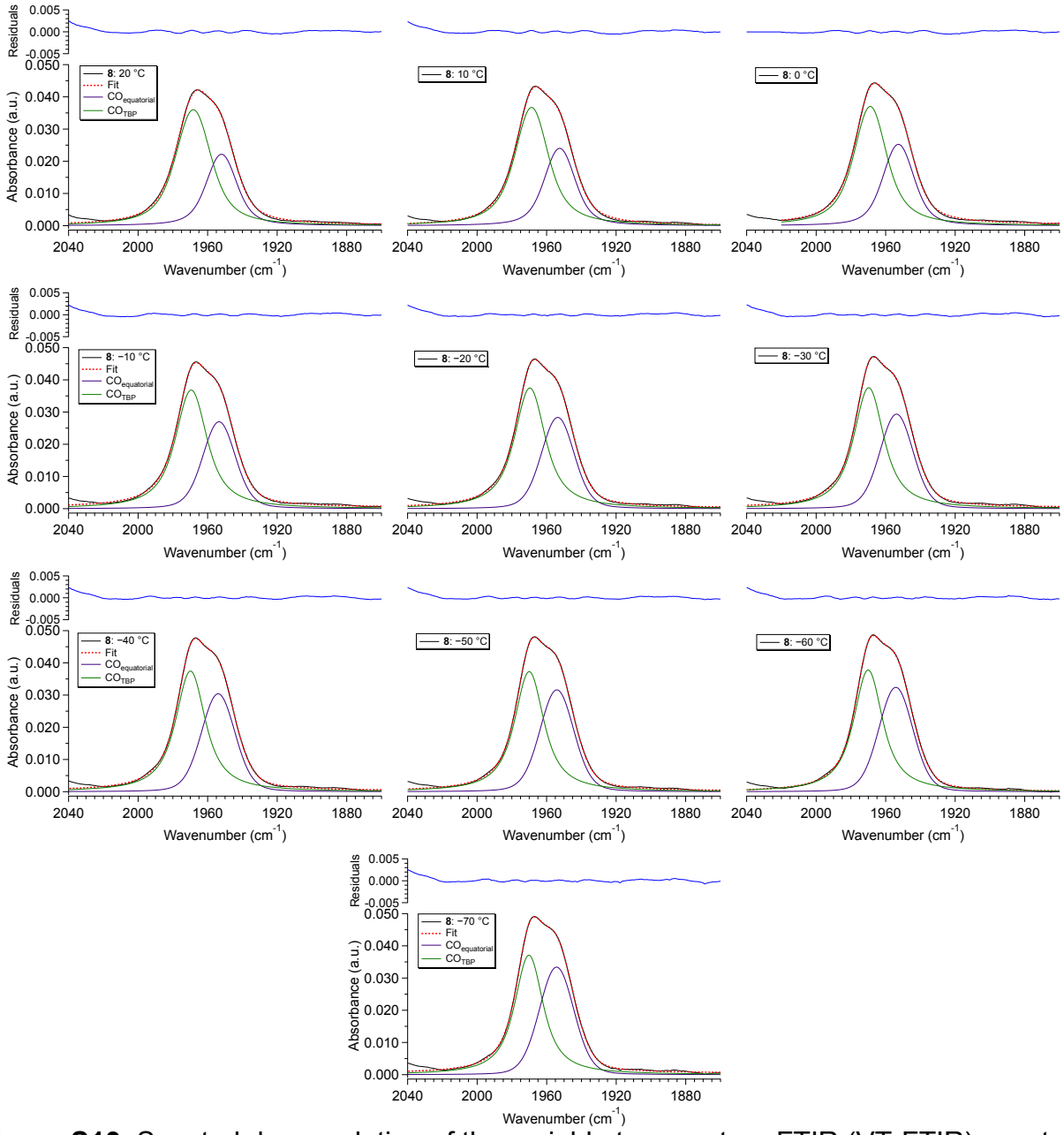

Figure S13. Spectral deconvolution of the variable temperature FTIR (VT-FTIR) spectra for complex **8**.

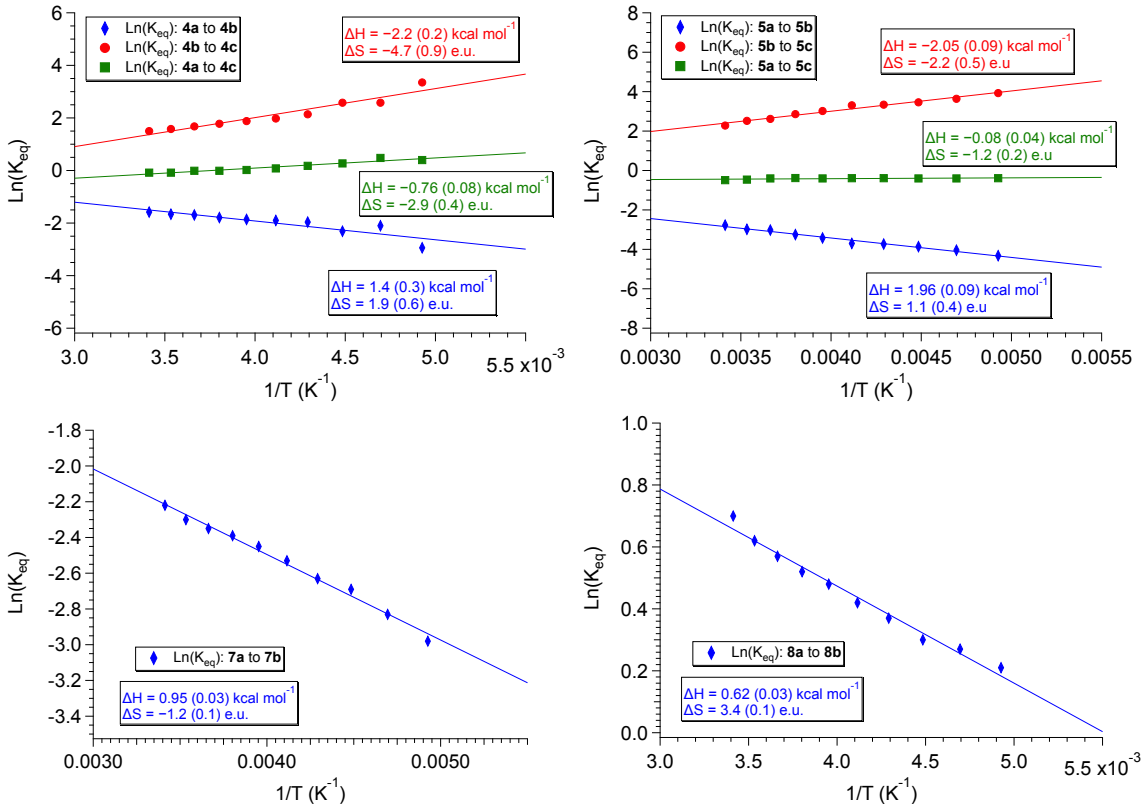

Figure S14. Van 't Hoff plots for complex **5** (left) and **7** (right) as determined from population ratios of the ν(CO) bands in the VT-FTIR. Equilibrium constants for isomerization from $CO_{equatorial}$ to CO_{axial} are shown as red traces, CO_{TBP} to CO_{axial} are shown as green traces, and $CO_{equatorial}$ to CO_{TBP} are shown as blue traces.

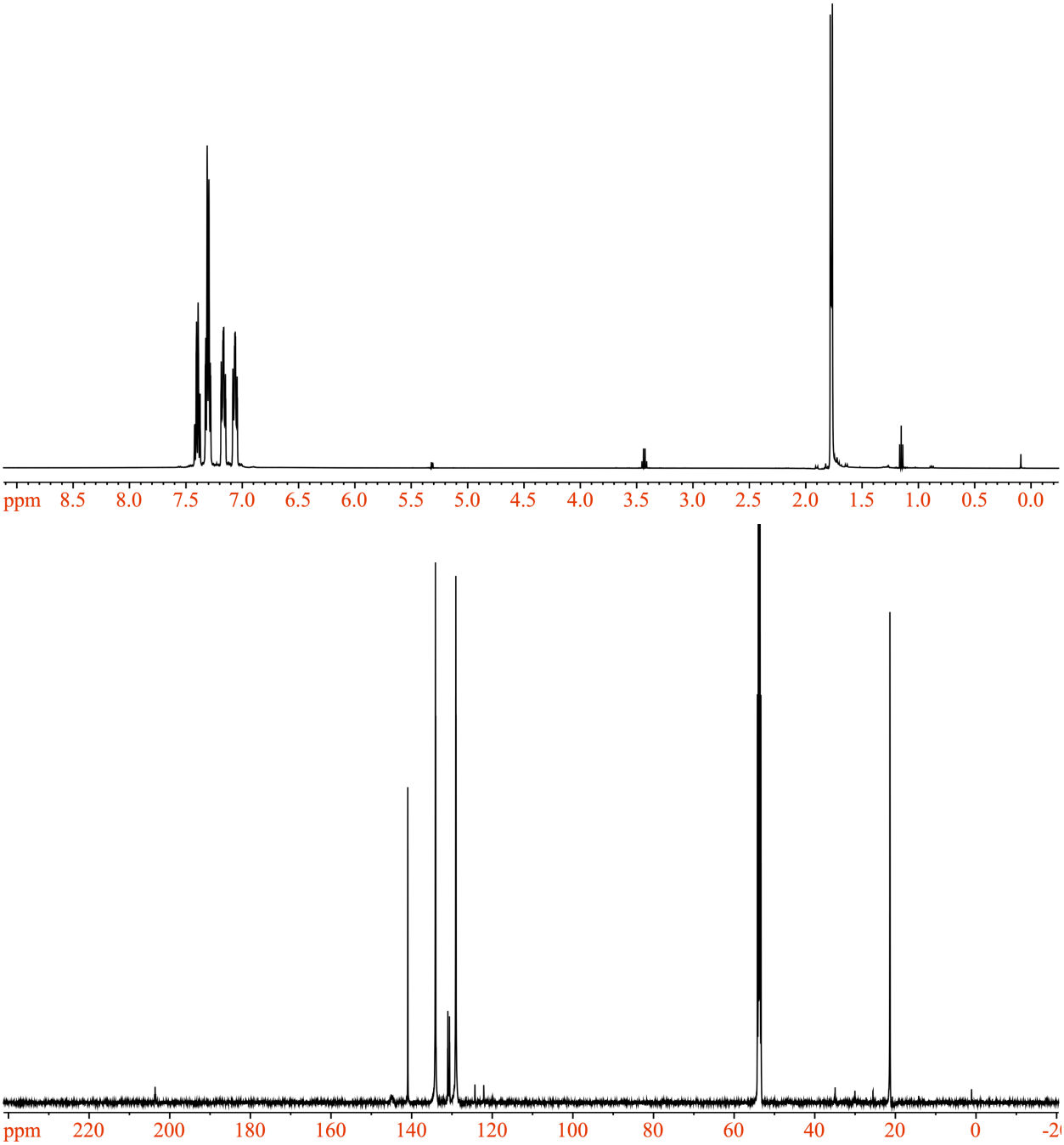

Figure S15. ^{1}H NMR (top) and ^{13}C NMR (bottom) of **2** in DCM-d_2 at 23 °C.

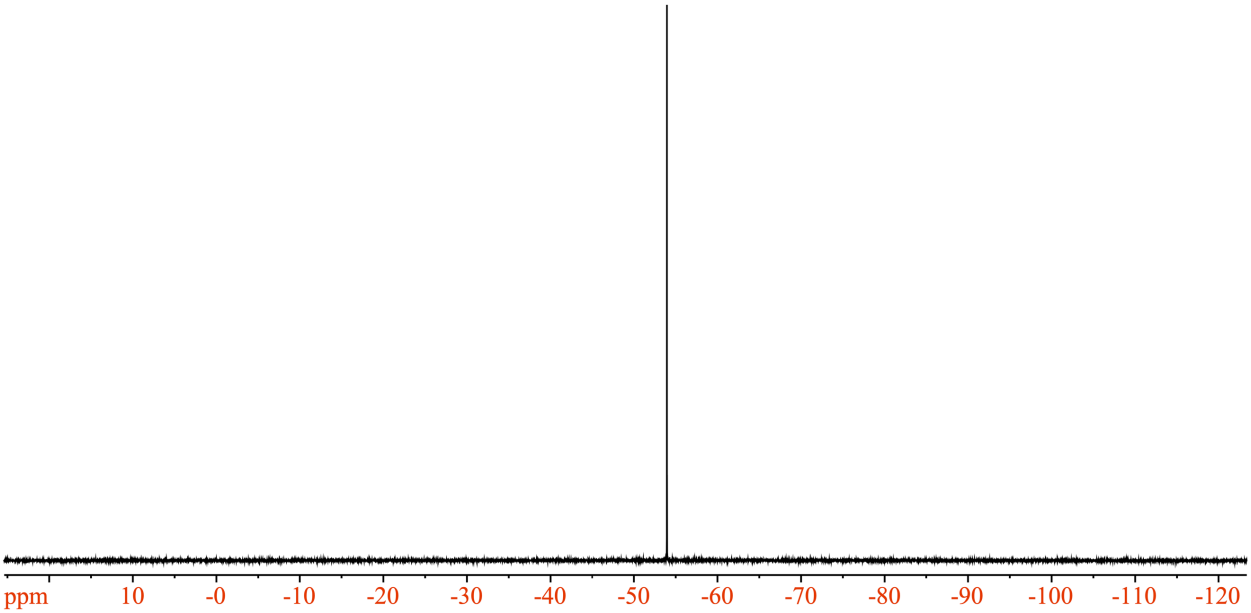

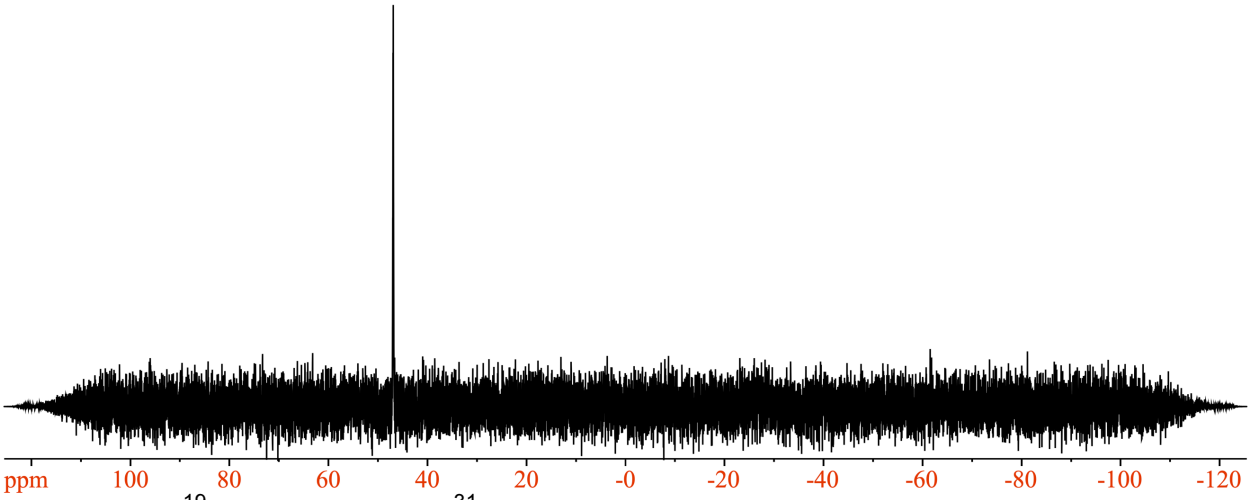

Figure S16. ^{19}F NMR (top) and ^{31}P NMR (bottom) of **2** in DCM-d_2 at 23 °C.

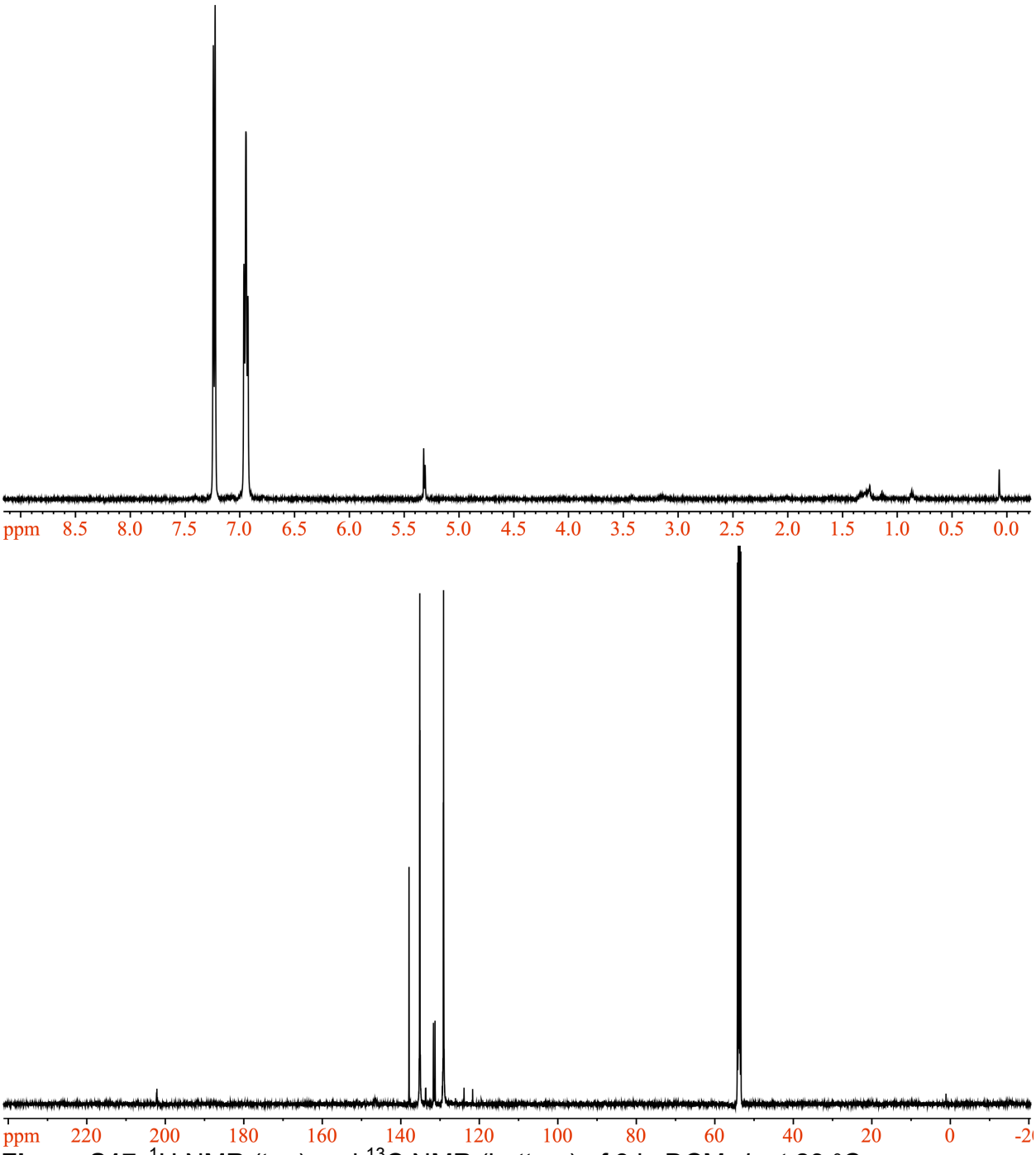

Figure S17. ^{1}H NMR (top) and ^{13}C NMR (bottom) of **3** in DCM-d_2 at 23 °C.

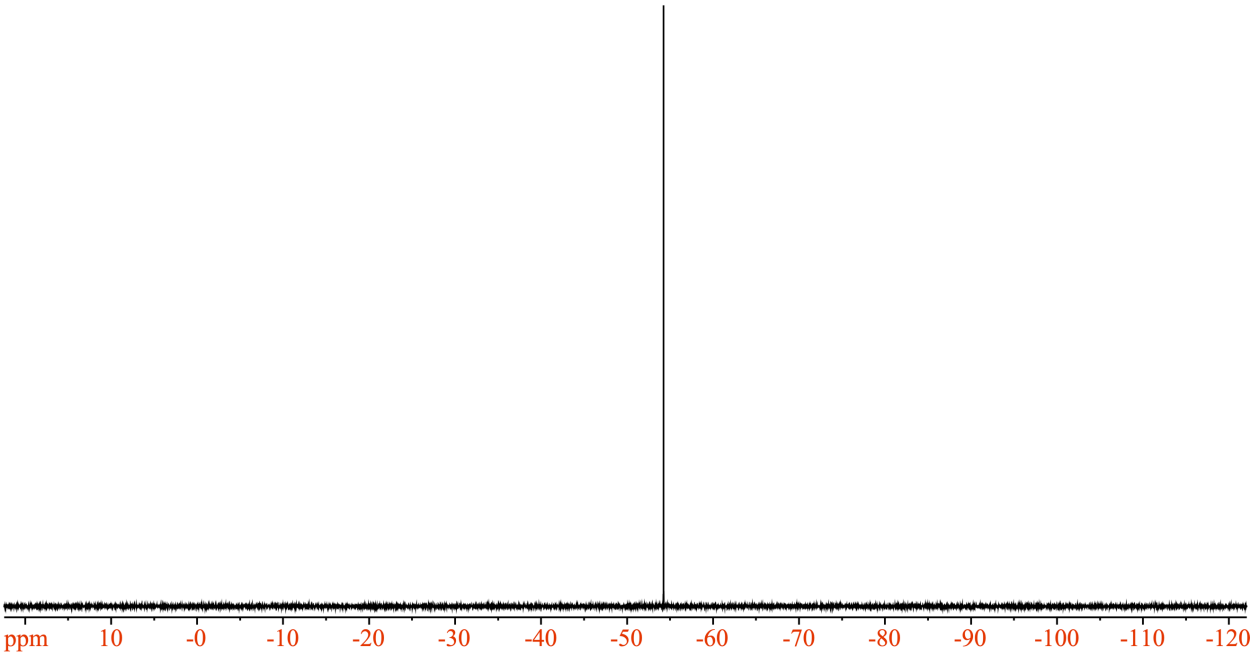

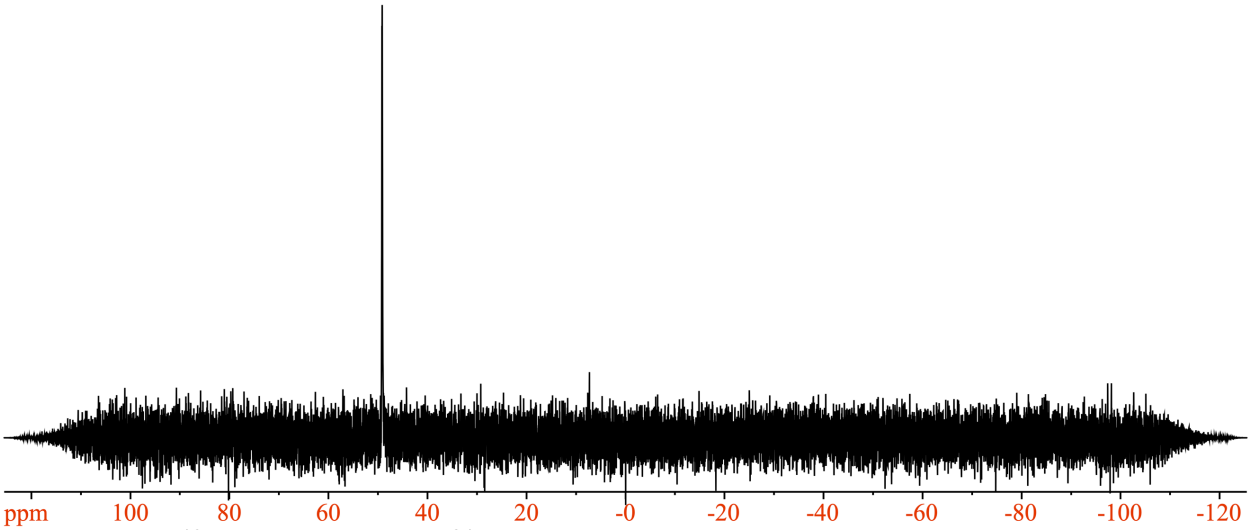

Figure S18. ^{19}F NMR (top) and ^{31}P NMR (bottom) of **3** in DCM-d_2 at 23 °C.

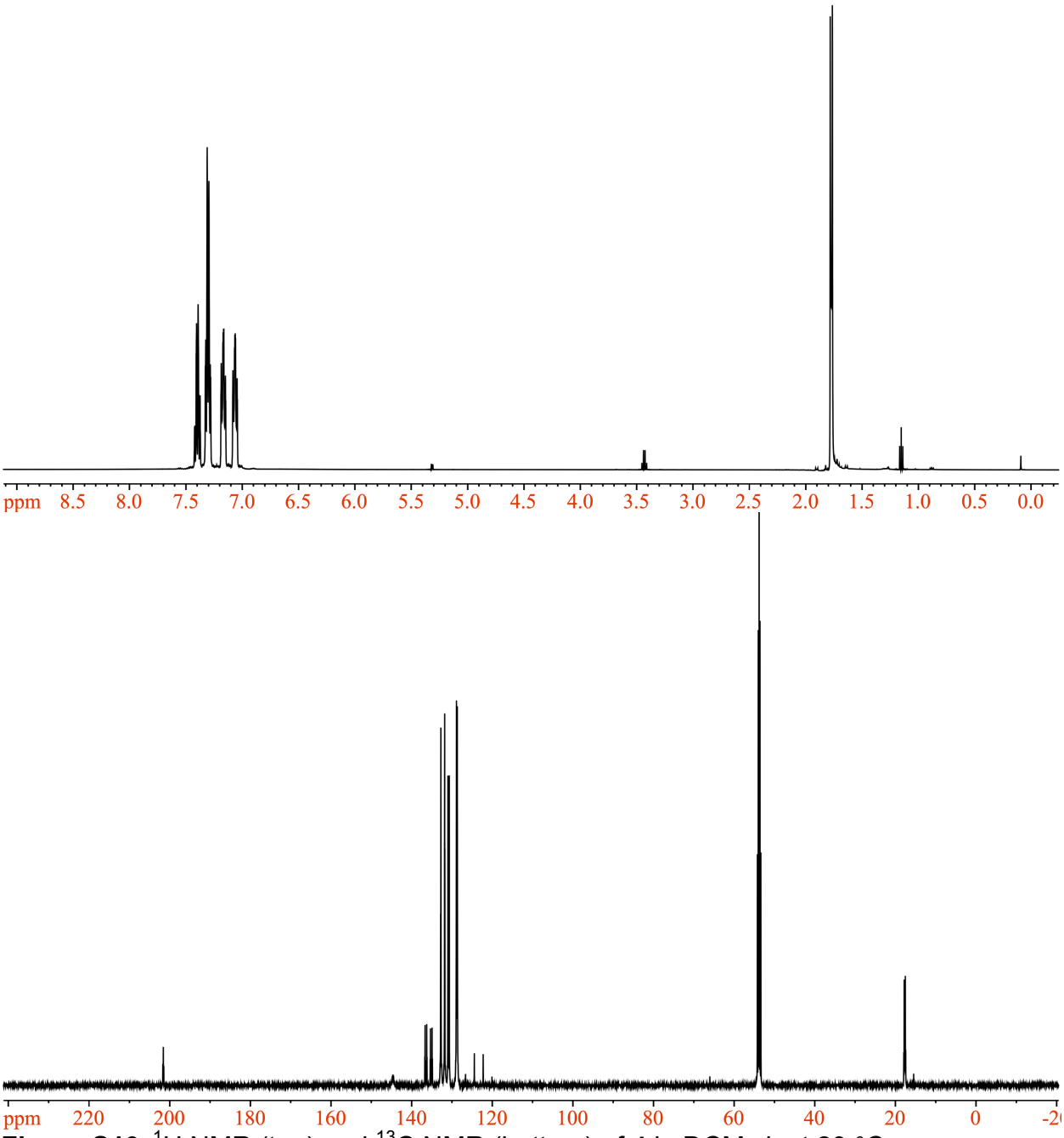

Figure S19. ^{1}H NMR (top) and ^{13}C NMR (bottom) of **4** in DCM-d_2 at 23 °C.

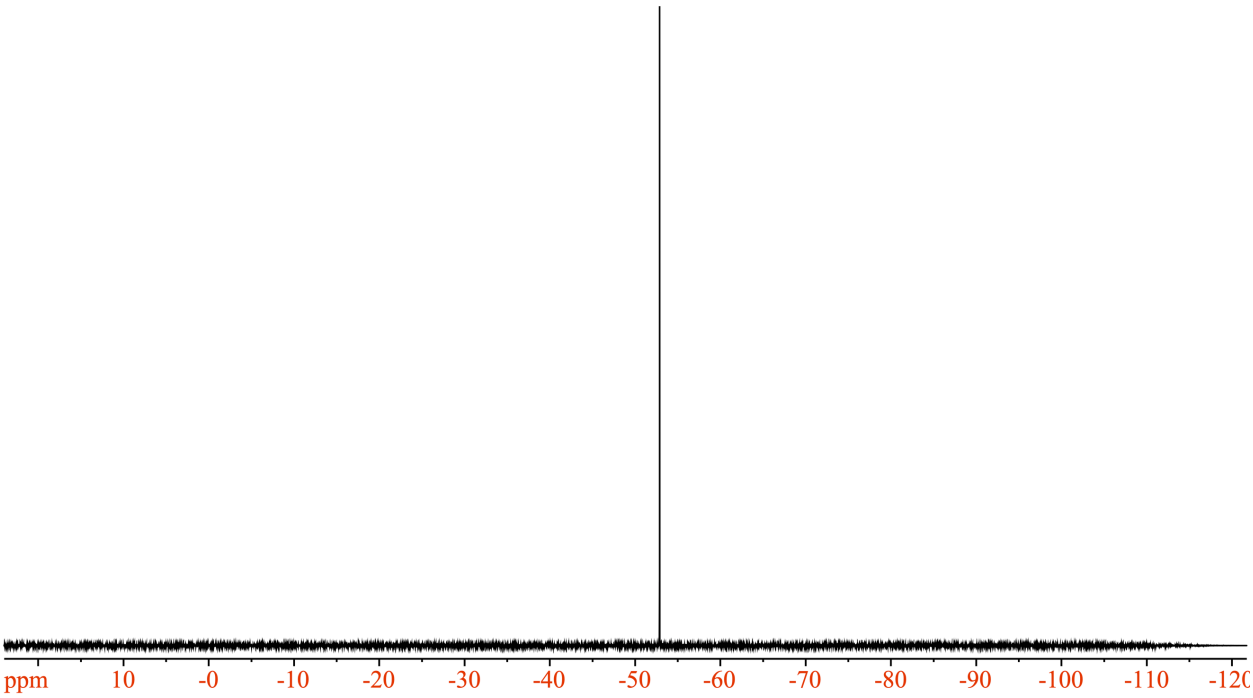

Figure S20. ^{19}F NMR (top) and ^{31}P NMR (bottom) of **4** in DCM-d_2 at 23 °C.

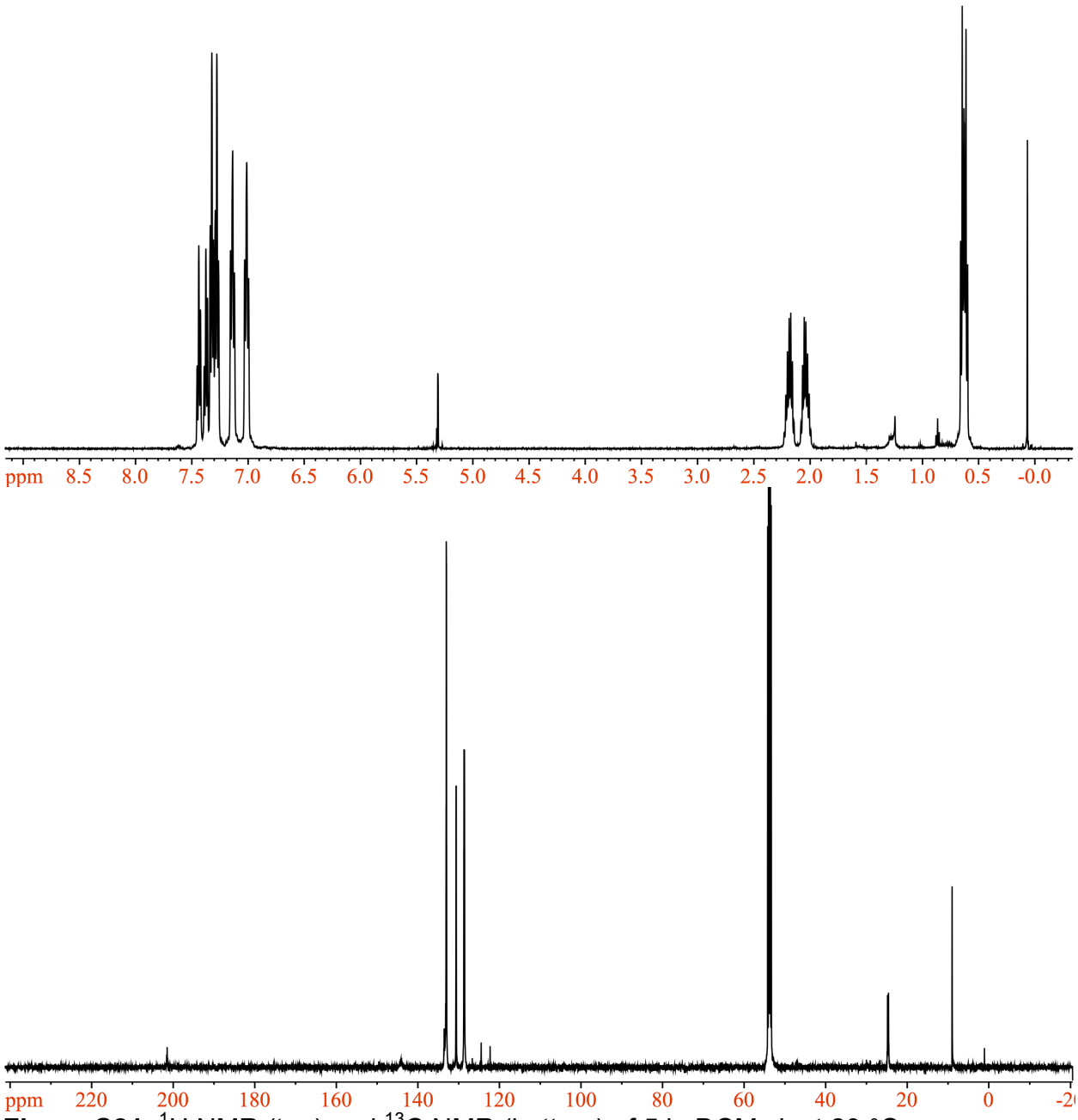

Figure S21. ^{1}H NMR (top) and ^{13}C NMR (bottom) of **5** in DCM-d_2 at 23 °C.

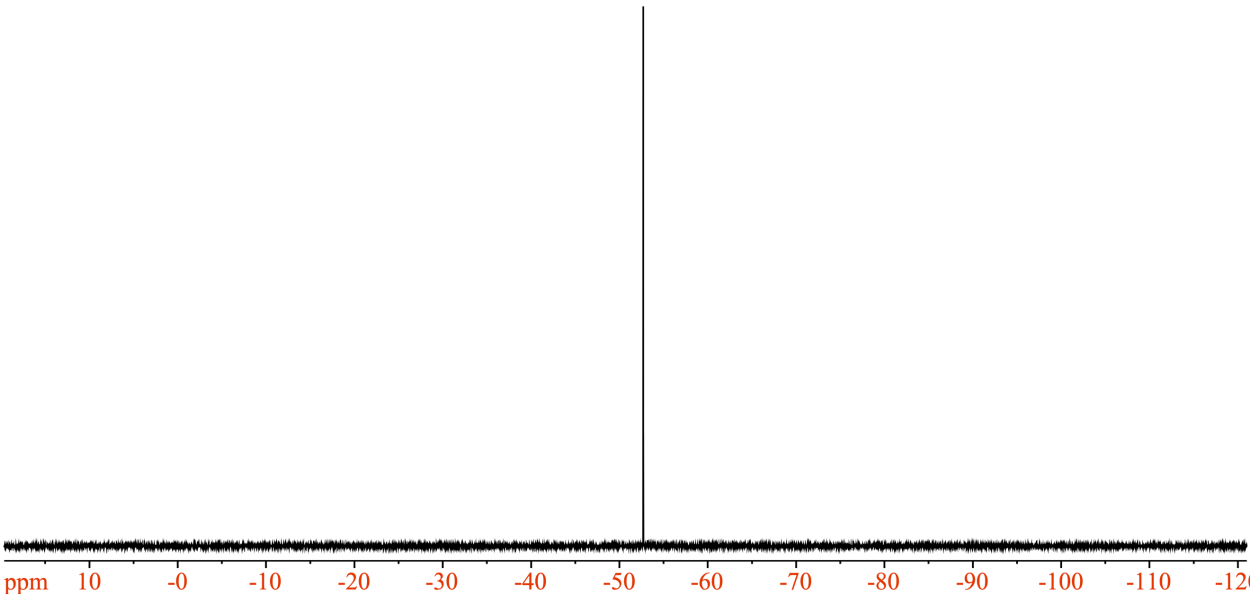

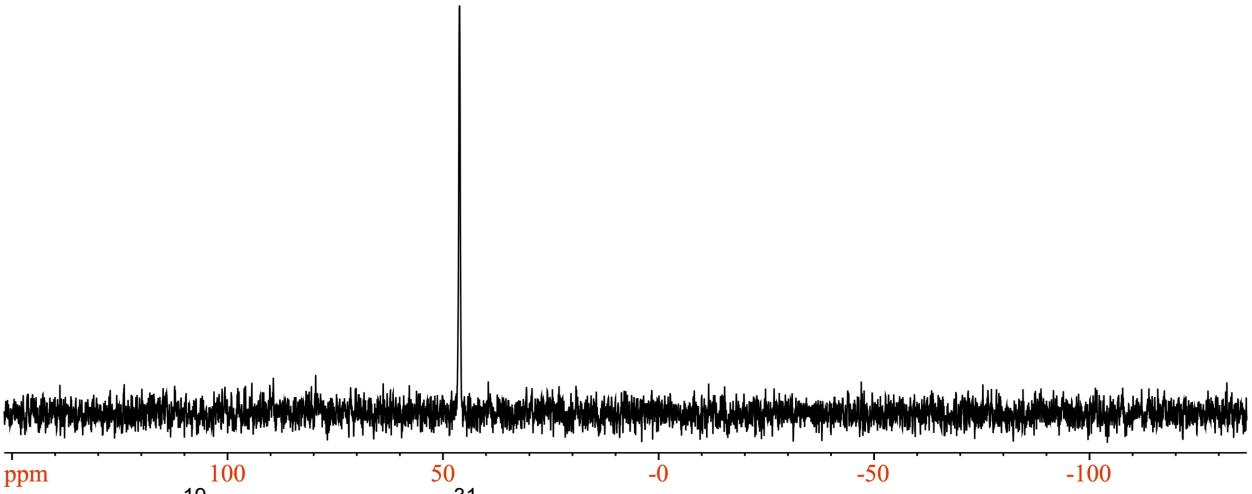

Figure S22. ^{19}F NMR (top) and ^{31}P NMR (bottom) of **5** in DCM-d_2 at 23 °C.

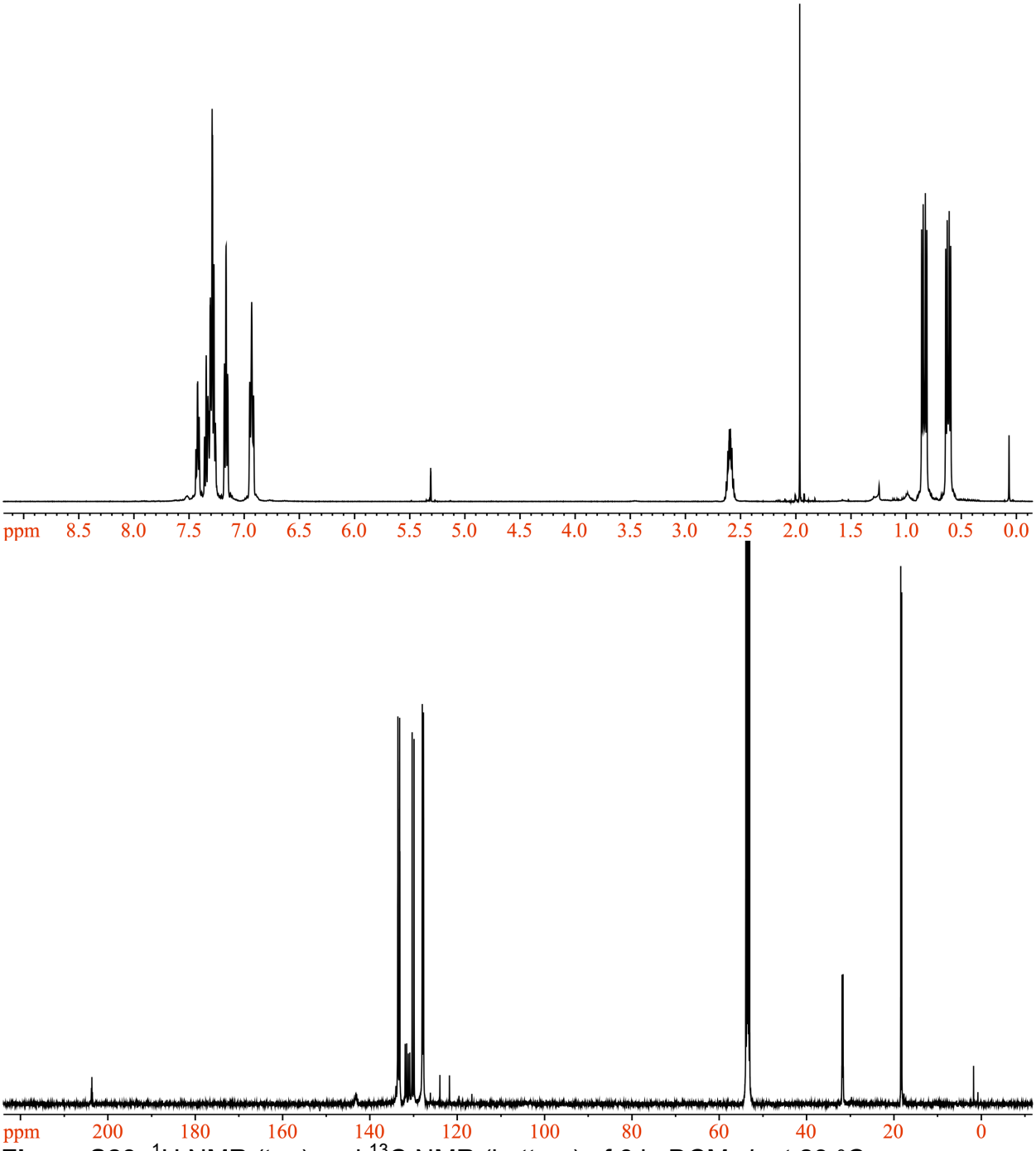

Figure S23. ^{1}H NMR (top) and ^{13}C NMR (bottom) of **6** in DCM-d_2 at 23 °C.

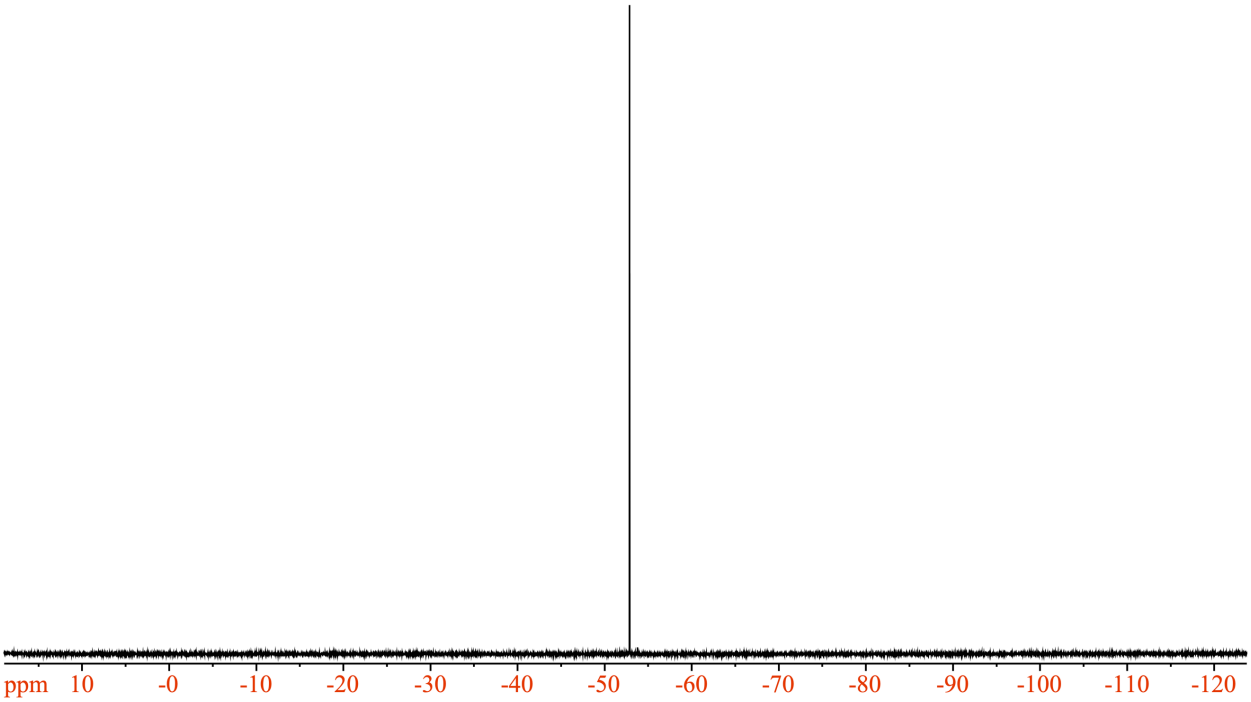

Figure S24. ^{19}F NMR (top) and ^{31}P NMR (bottom) of **6** in DCM-d_2 at 23 °C.

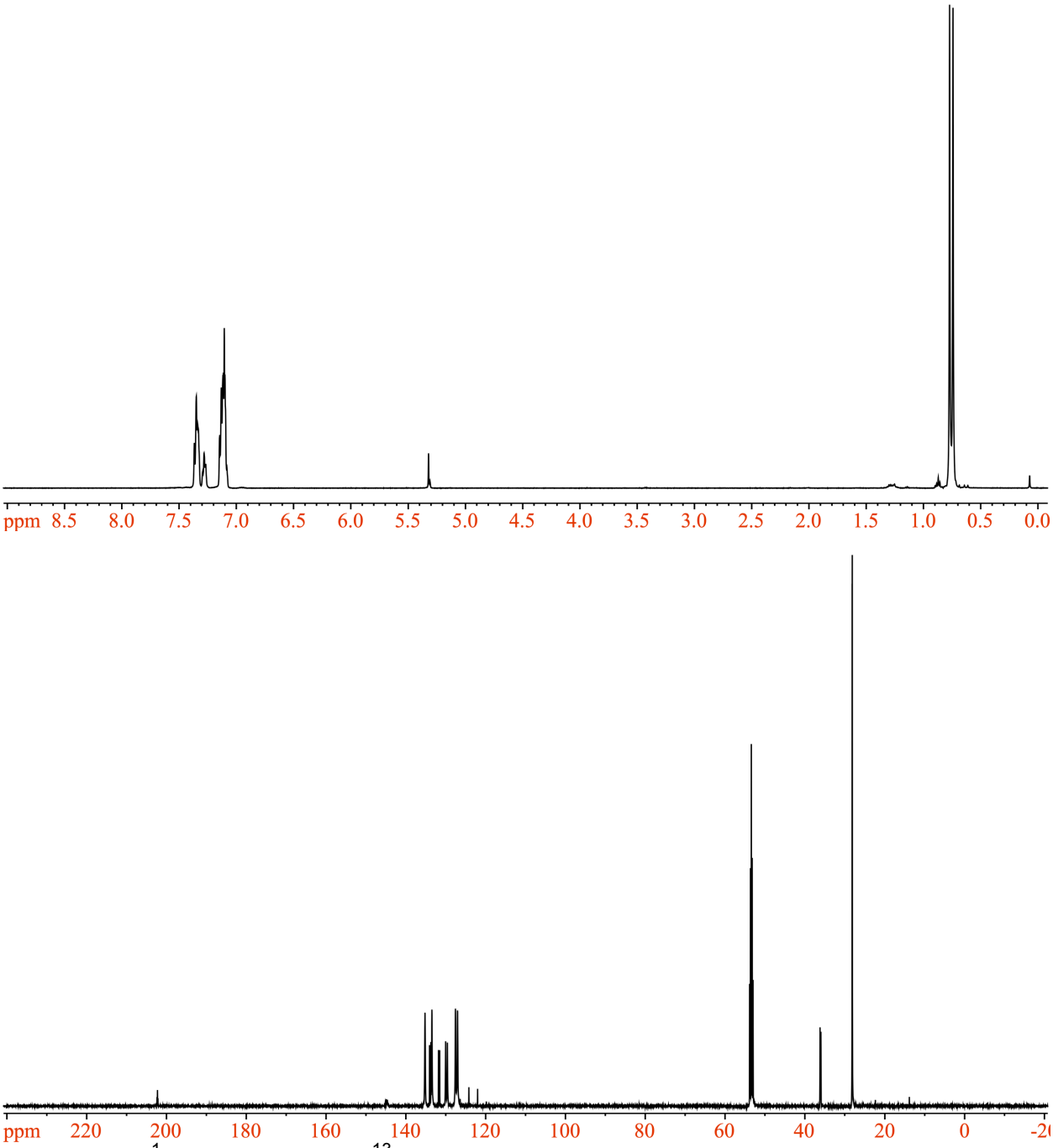

Figure S25. ^{1}H NMR (top) and ^{13}C NMR (bottom) of **7** in DCM-d_2 at 23 °C.

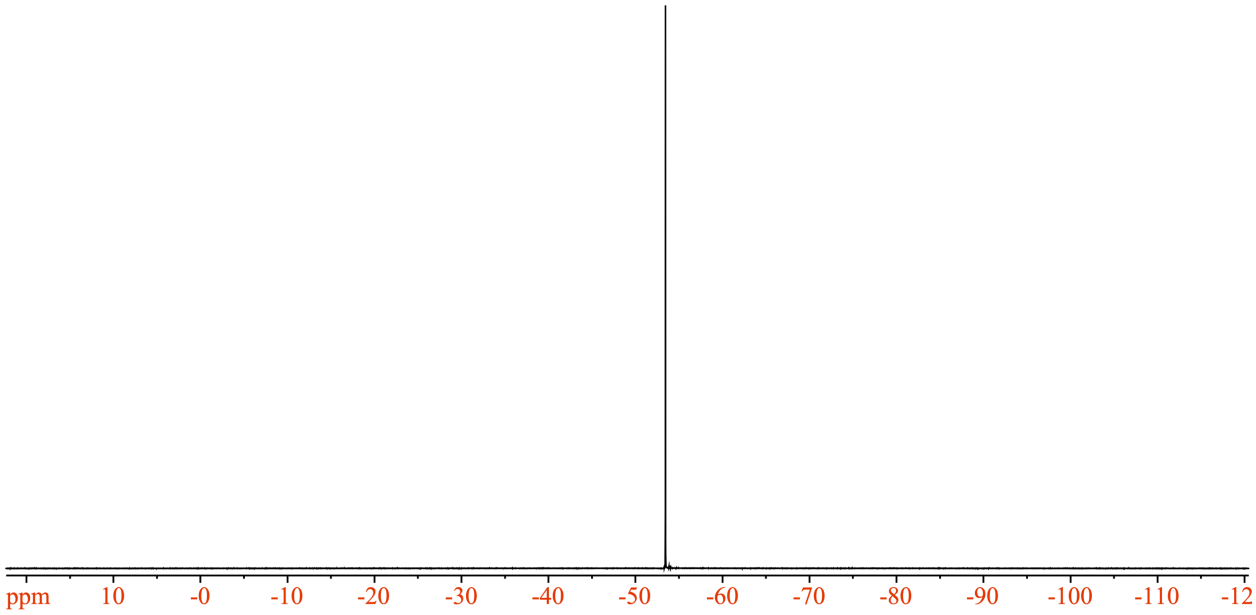

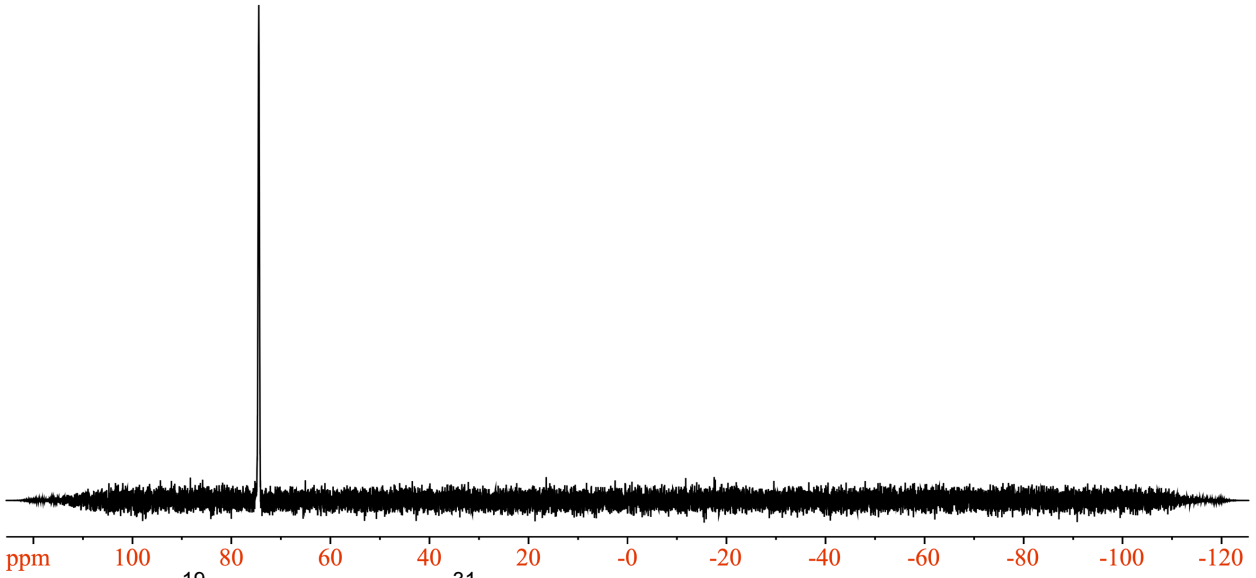

Figure S26. ^{19}F NMR (top) and ^{31}P NMR (bottom) of **7** in DCM-d_2 at 23 °C.

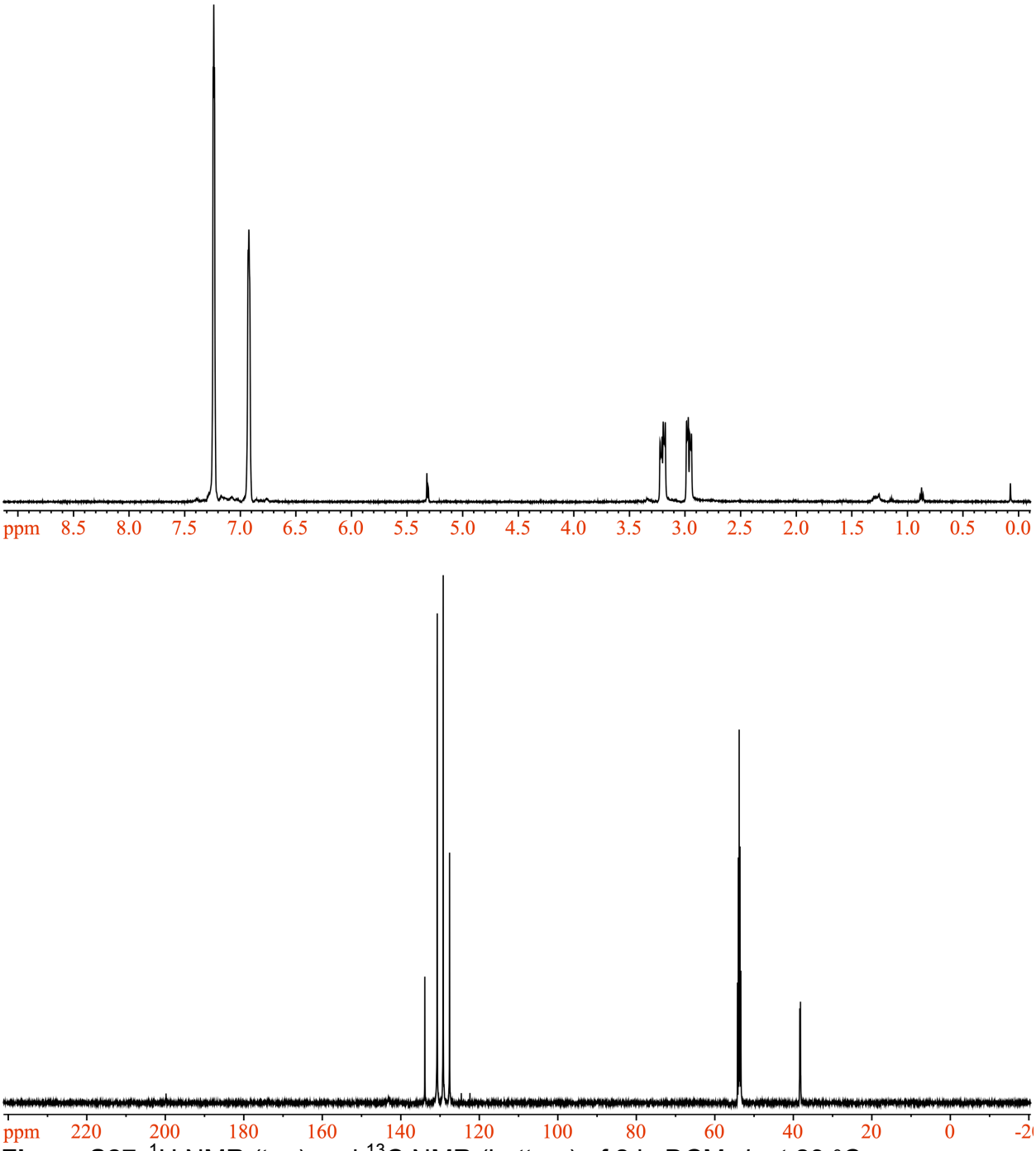

Figure S27. ^{1}H NMR (top) and ^{13}C NMR (bottom) of **8** in DCM-d_2 at 23 °C.

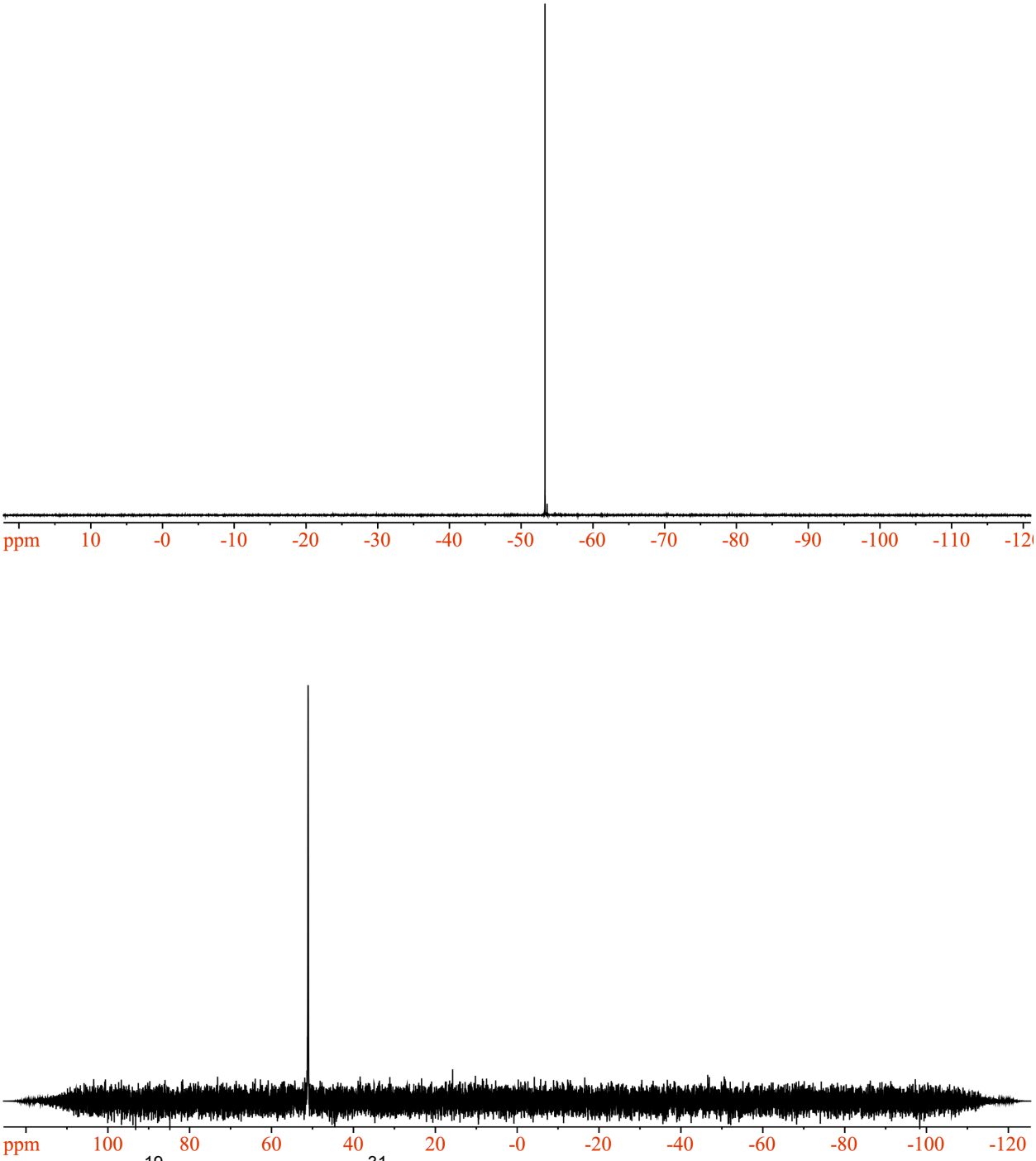

Figure S28. ^{19}F NMR (top) and ^{31}P NMR (bottom) of **8** in DCM-d_2 at 23 °C.

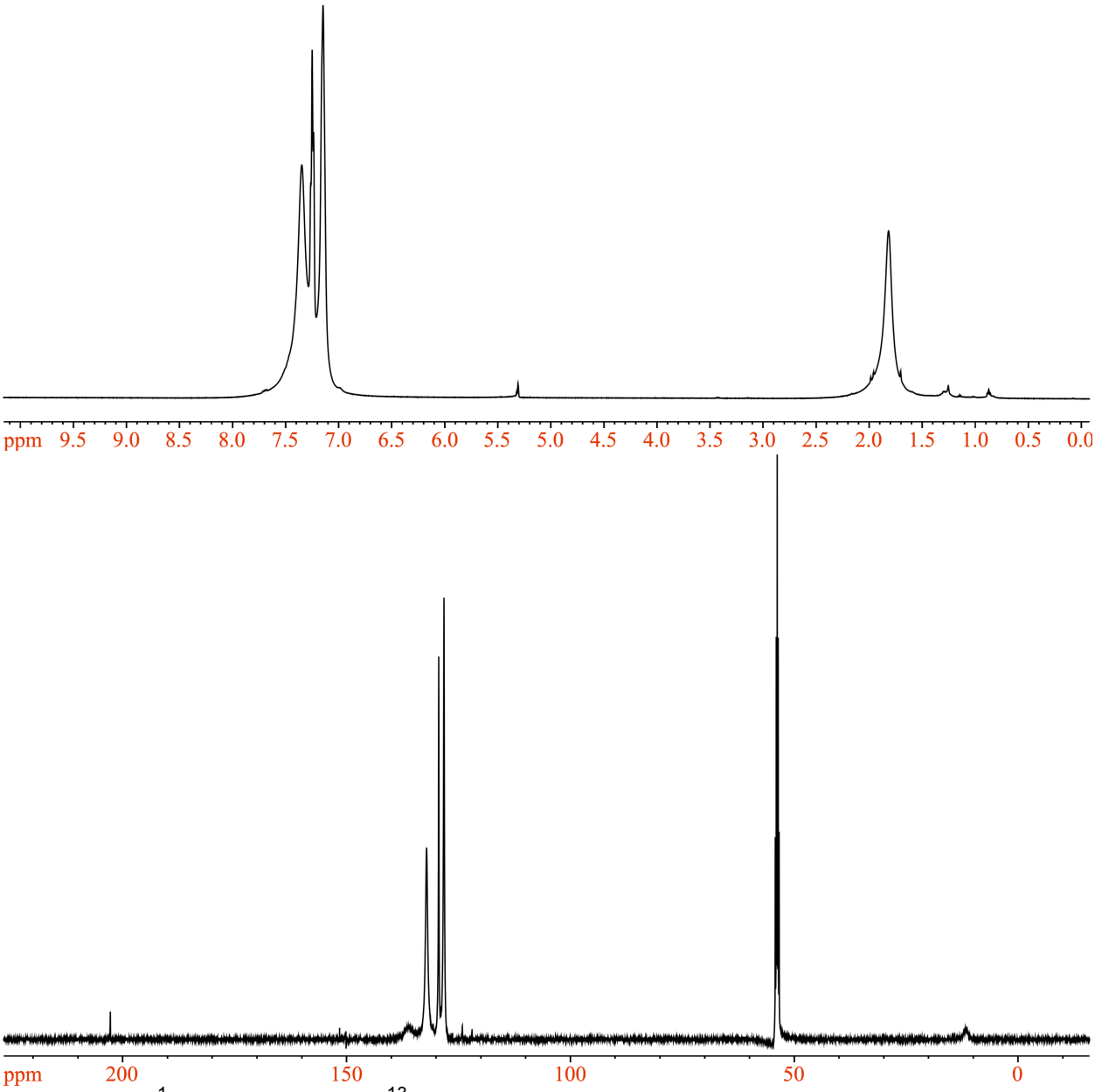

Figure S29. ^{1}H NMR (top) and ^{13}C NMR (bottom) of **9** in DCM-d_2 at 23 °C.

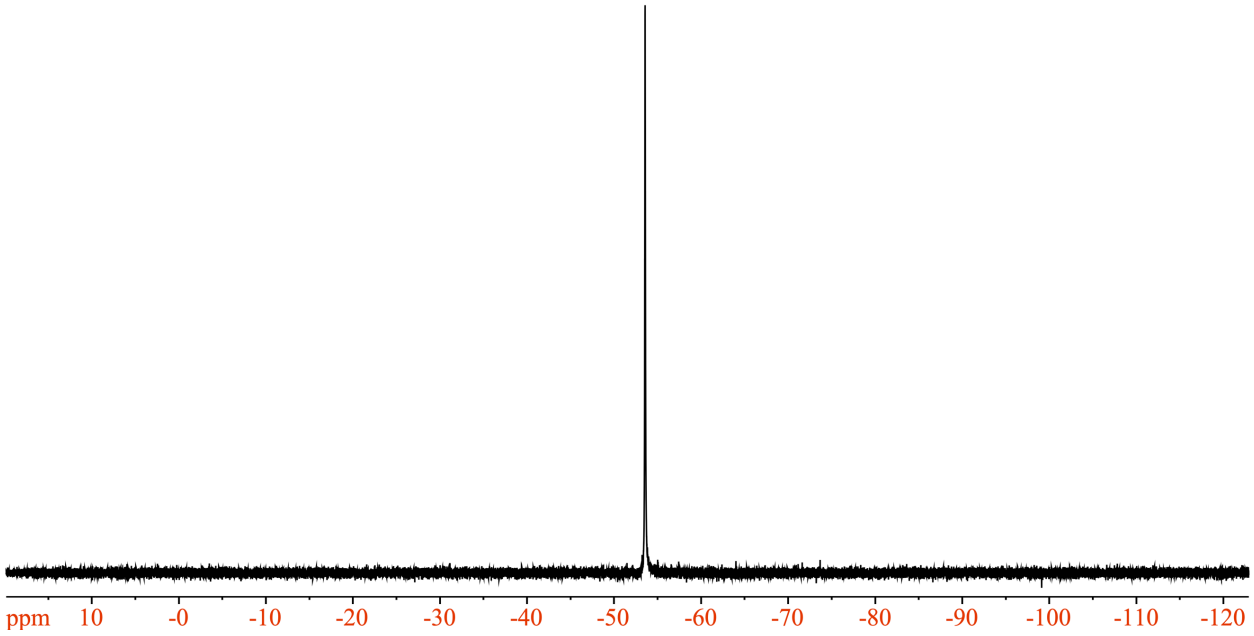

Figure S30. ^{19}F NMR (top) and ^{31}P NMR (bottom) of **8** in DCM-d_2 at 23 °C.

Table S1. Structural and refinement data for complex **2** (CSD: 1895688).

Empirical formula	$C_{48}H_{44}Cl_2F_6OP_2RuS_2$
Formula weight	1048.86
Temperature/K	100.0
Crystal system	monoclinic
Space group	$P2_1/n$
a/Å	22.0285(3)
b/Å	10.09770(10)
c/Å	22.3884(3)
α/°	90
β/°	108.0770(10)
γ/°	90
Volume/Å^3	4734.20(11)
Z	4
ρ_{calc}g/cm^3	1.472
μ/mm^{-1}	0.659
F(000)	2136.0
Crystal size/mm^3	0.2 × 0.2 × 0.2
Radiation	MoKα (λ = 0.71073)
2Θ range for data collection/°	2.266 to 50.7
Index ranges	-26 ≤ h ≤ 26, -12 ≤ k ≤ 12, -26 ≤ l ≤ 25
Reflections collected	51983
Independent reflections	8669 [R_{int} = 0.0324, R_{sigma} = 0.0213]
Data/restraints/parameters	8669/17/575
Goodness-of-fit on F^2	1.046
Final R indexes [I>=2σ (I)]	R_1 = 0.0367, wR_2 = 0.0955
Final R indexes [all data]	R_1 = 0.0419, wR_2 = 0.1012
Largest diff. peak/hole / e Å^{-3}	2.77/-0.73

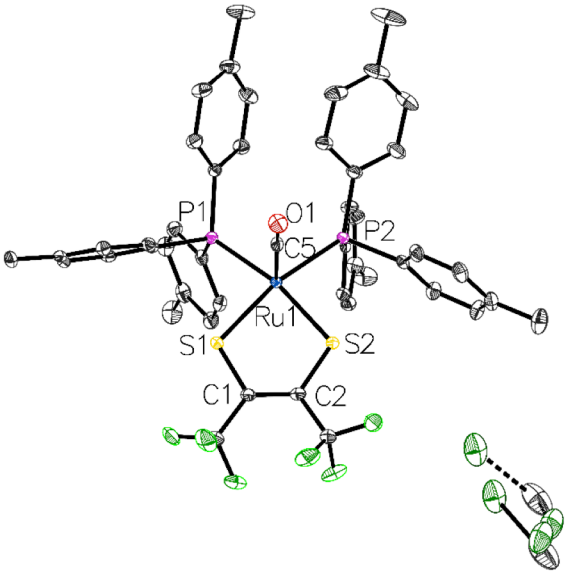

Notes on refinement: One molecule of dichloromethane exhibits significant positional disorder in the unit cell. This was treated as two-site disorder, modeled and refined anisotropically with carbon-chlorine and chlorine-chlorine distances constrained.

Table S2. Structural and refinement data for complex **3** (CSD: 1895689).

Empirical formula	$C_{43}H_{28}Cl_{10}F_6OP_2RuS_2$
Formula weight	1256.28
Temperature/K	100.0
Crystal system	triclinic
Space group	P-1
a/Å	11.3432(4)
b/Å	12.7836(5)
c/Å	17.7908(7)
α/°	82.7760(10)
β/°	78.0010(10)
γ/°	75.6050(10)
Volume/Å^3	2436.72(16)
Z	2
ρ_{calc}g/cm^3	1.712
μ/mm^{-1}	1.080
F(000)	1248.0
Crystal size/mm^3	0.2 × 0.2 × 0.1
Radiation	MoKα (λ = 0.71073)
2Θ range for data collection/°	3.3 to 52.904
Index ranges	-14 ≤ h ≤ 14, -15 ≤ k ≤ 15, -22 ≤ l ≤ 22
Reflections collected	34329
Independent reflections	10022 [R_{int} = 0.0319, R_{sigma} = 0.0332]
Data/restraints/parameters	10022/0/586
Goodness-of-fit on F^2	1.040
Final R indexes [I>=2σ (I)]	R_1 = 0.0445, wR_2 = 0.1104
Final R indexes [all data]	R_1 = 0.0525, wR_2 = 0.1166
Largest diff. peak/hole / e Å^{-3}	2.52/-1.97

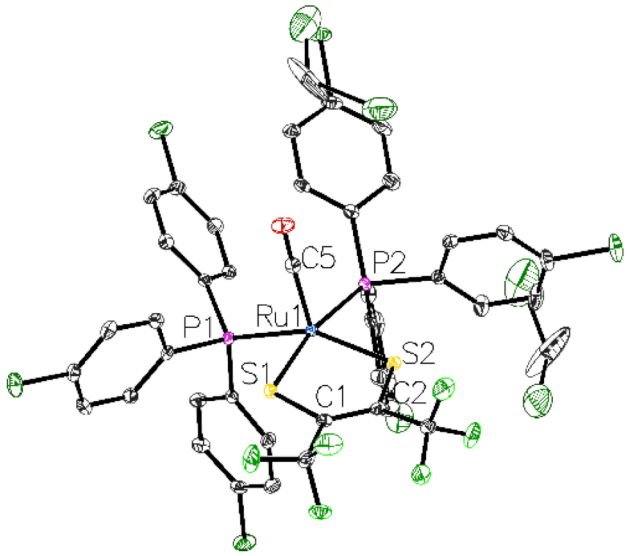

Table S3. Structural and refinement data for complex **4** (CSD: 1895690).

Empirical formula	$C_{31}H_{26}F_6OP_2RuS_2$
Formula weight	755.65
Temperature/K	100.0
Crystal system	monoclinic
Space group	$P2_1/n$
a/Å	9.9248(5)
b/Å	14.4285(7)
c/Å	22.0349(12)
α/°	90
β/°	93.158(2)
γ/°	90
Volume/Å^3	3150.6(3)
Z	4
ρ_{calc}g/cm^3	1.593
μ/mm^{-1}	0.792
F(000)	1520.0
Crystal size/mm^3	0.2 × 0.2 × 0.1
Radiation	MoKα (λ = 0.71073)
2Θ range for data collection/°	3.376 to 52.768
Index ranges	-12 ≤ h ≤ 12, -17 ≤ k ≤ 18, -27 ≤ l ≤ 27
Reflections collected	12342
Independent reflections	6439 [R_{int} = 0.0231, R_{sigma} = 0.0334]
Data/restraints/parameters	6439/0/412
Goodness-of-fit on F^2	1.033
Final R indexes [I>=2σ (I)]	R_1 = 0.0355, wR_2 = 0.0759
Final R indexes [all data]	R_1 = 0.0463, wR_2 = 0.0801
Largest diff. peak/hole / e Å^{-3}	0.91/-0.75

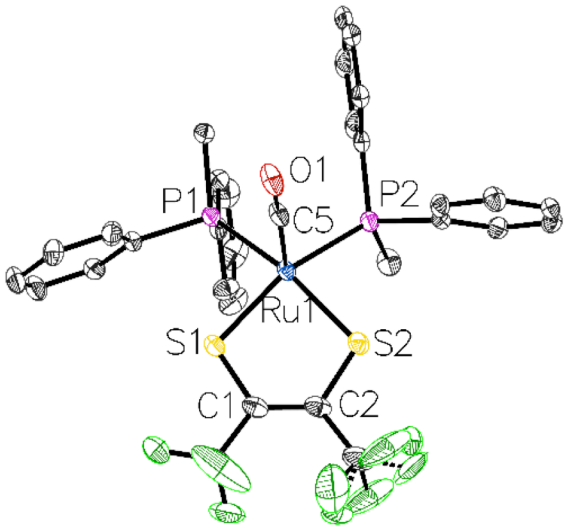

Notes on refinement: Rotational disorder exists about the C3 axis of one of the CF_3 of the dithiolene ligand; this was treated as two-site positional disorder, modeled and refined anisotropically.

Table S4. Structural and refinement data for complex **5** (CSD: 1895691).

Empirical formula	$C_{33}H_{30}F_6OP_2RuS_2$
Formula weight	783.70
Temperature/K	100.0
Crystal system	monoclinic
Space group	$P2_1/n$
a/Å	10.1017(13)
b/Å	14.5492(18)
c/Å	22.325(3)
α/°	90
β/°	92.279(2)
γ/°	90
Volume/Å^3	3278.5(7)
Z	4
ρ_{calc}g/cm^3	1.588
μ/mm^{-1}	0.764
F(000)	1584.0
Crystal size/mm^3	0.3 × 0.1 × 0.1
Radiation	MoKα (λ = 0.71073)
2Θ range for data collection/°	3.342 to 51.432
Index ranges	-12 ≤ h ≤ 12, -17 ≤ k ≤ 17, -27 ≤ l ≤ 27
Reflections collected	31464
Independent reflections	31464 [R_{int} = , R_{sigma} = 0.0384]
Data/restraints/parameters	31464/0/437
Goodness-of-fit on F^2	1.067
Final R indexes [I>=2σ (I)]	R_1 = 0.0294, wR_2 = 0.0676
Final R indexes [all data]	R_1 = 0.0328, wR_2 = 0.0689
Largest diff. peak/hole / e Å^{-3}	0.49/-0.37

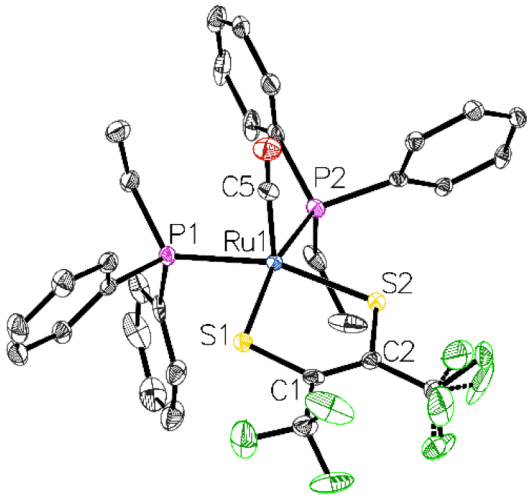

Notes on refinement: Two contributing twin components exist and were treated with the PLATON routine Twin.Rot.Mat and subsequently refined within the Olex2 software. Rotational disorder exists about the C3 axis of one of the CF_3 of the dithiolene ligand; this was treated as two-site positional disorder, modeled and refined anisotropically.

Table S5. Structural and refinement data for complex **6** (CSD: 1895696).

Empirical formula	$C_{39}H_{40}F_6N_2OP_2RuS_2$
Formula weight	893.86
Temperature/K	100.0
Crystal system	triclinic
Space group	P-1
a/Å	11.3418(6)
b/Å	12.3720(6)
c/Å	15.6817(8)
α/°	82.532(2)
β/°	88.038(2)
γ/°	87.632(2)
Volume/Å^3	2179.01(19)
Z	2
ρ_{calc}g/cm^3	1.362
μ/mm^{-1}	0.585
F(000)	912.0
Crystal size/mm^3	0.2 × 0.2 × 0.1
Radiation	MoKα (λ = 0.71073)
2Θ range for data collection/°	4.49 to 51.388
Index ranges	-13 ≤ h ≤ 10, -15 ≤ k ≤ 14, -19 ≤ l ≤ 19
Reflections collected	29765
Independent reflections	8242 [R_{int} = 0.0391, R_{sigma} = 0.0464]
Data/restraints/parameters	8242/0/540
Goodness-of-fit on F^2	1.022
Final R indexes [I>=2σ (I)]	R_1 = 0.0347, wR_2 = 0.0684
Final R indexes [all data]	R_1 = 0.0497, wR_2 = 0.0728
Largest diff. peak/hole / e Å^{-3}	0.52/-0.64

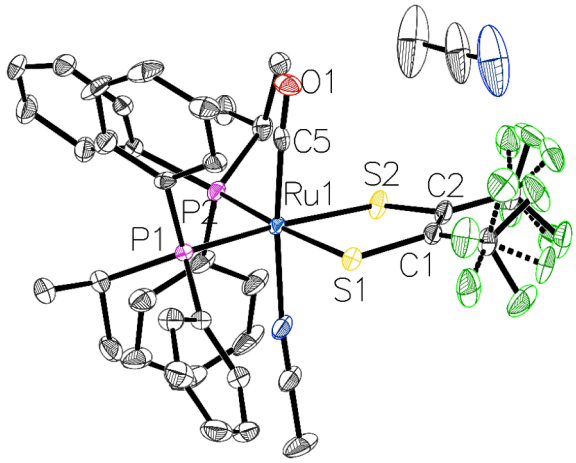

Notes on refinement: Rotational disorder exists about the C3 axis of one of the CF_3 groups of the dithiolene ligand; this was treated as two-site positional disorder, modeled and refined anisotropically. Density attributed to a second highly disordered molecule of uncoordinated acetonitrile was omitted from the unit cell using the PLATON routine SQUEEZE.

Table S6. Structural and refinement data for complex **7** (CSD: 1895697).

Empirical formula	$C_{38}H_{40}Cl_2F_6OP_2RuS_2$
Formula weight	924.73
Temperature/K	100.0
Crystal system	triclinic
Space group	P-1
a/Å	9.6923(10)
b/Å	13.9409(13)
c/Å	15.7231(15)
α/°	69.532(3)
β/°	89.543(3)
γ/°	80.855(3)
Volume/Å^3	1962.5(3)
Z	2
ρ_{calc}g/cm^3	1.565
μ/mm^{-1}	0.783
F(000)	940.0
Crystal size/mm^3	0.3 × 0.1 × 0.1
Radiation	MoKα (λ = 0.71073)
2Θ range for data collection/°	2.768 to 52.742
Index ranges	-12 ≤ h ≤ 12, -17 ≤ k ≤ 17, -19 ≤ l ≤ 19
Reflections collected	49727
Independent reflections	8021 [R_{int} = 0.0588, R_{sigma} = 0.0448]
Data/restraints/parameters	8021/0/475
Goodness-of-fit on F^2	1.019
Final R indexes [I>=2σ (I)]	R_1 = 0.0308, wR_2 = 0.0607
Final R indexes [all data]	R_1 = 0.0460, wR_2 = 0.0664
Largest diff. peak/hole / e Å^{-3}	0.70/-0.58

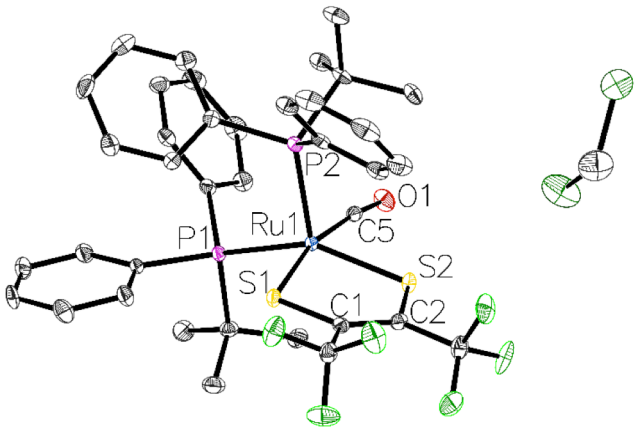

Table S7. Structural and refinement data for complex **8** (CSD: 1895698).

Empirical formula	$C_{47}H_{42}F_6OP_2RuS_2$
Formula weight	963.93
Temperature/K	100.0
Crystal system	monoclinic
Space group	$P2_1/n$
a/Å	19.0916(12)
b/Å	13.4073(8)
c/Å	20.9793(11)
α/°	90
β/°	116.859(2)
γ/°	90
Volume/Å^3	4790.7(5)
Z	4
ρ_{calc}g/cm^3	1.336
μ/mm^{-1}	0.537
F(000)	1968.0
Crystal size/mm^3	0.3 × 0.2 × 0.1
Radiation	MoKα (λ = 0.71073)
2Θ range for data collection/°	3.736 to 50.7
Index ranges	-22 ≤ h ≤ 22, -16 ≤ k ≤ 16, -21 ≤ l ≤ 25
Reflections collected	55591
Independent reflections	8759 [R_{int} = 0.0577, R_{sigma} = 0.0481]
Data/restraints/parameters	8759/130/585
Goodness-of-fit on F^2	1.071
Final R indexes [I>=2σ (I)]	R_1 = 0.0587, wR_2 = 0.1326
Final R indexes [all data]	R_1 = 0.0858, wR_2 = 0.1445
Largest diff. peak/hole / e Å^{-3}	3.42/-0.73

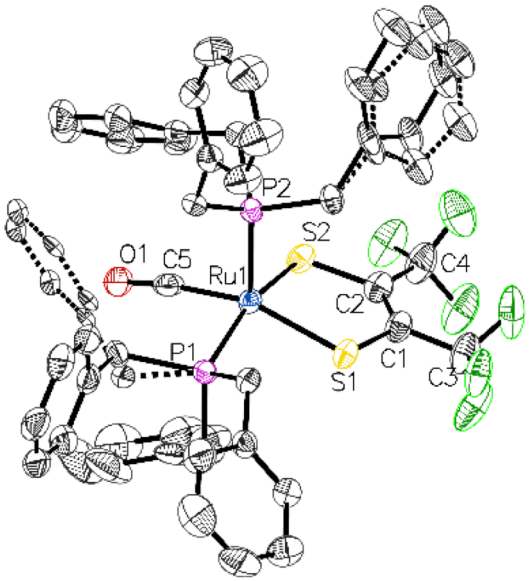

Notes on refinement: Two orientations exist at two of the benzyl moieties. This results in significant disorder which was treated as two-site positional disorder with RIGU and EADP constraints on the benzyl rings. Furthermore, density attributed to a highly disordered molecule of dichloromethane was omitted from the unit cell using the PLATON routine SQUEEZE.

Table S8. Structural and refinement data for complex **9** (CSD: 1895699).

Empirical formula	$C_{45}H_{41}Cl_2F_6OP_3RuS_2$
Formula weight	1040.78
Temperature/K	100.0
Crystal system	monoclinic
Space group	$P2_1/c$
a/Å	11.4007(3)
b/Å	23.5110(5)
c/Å	17.6024(4)
α/°	90
β/°	108.7530(10)
γ/°	90
Volume/Å^3	4467.71(18)
Z	4
ρ_{calc}g/cm^3	1.547
μ/mm^{-1}	6.350
F(000)	2112.0
Crystal size/mm^3	0.2 × 0.2 × 0.2
Radiation	CuKα (λ = 1.54178)
2Θ range for data collection/°	6.5 to 140.554
Index ranges	-13 ≤ h ≤ 13, -27 ≤ k ≤ 28, -21 ≤ l ≤ 21
Reflections collected	32908
Independent reflections	8476 [R_{int} = 0.0493, R_{sigma} = 0.0410]
Data/restraints/parameters	8476/0/544
Goodness-of-fit on F^2	1.022
Final R indexes [I>=2σ (I)]	R_1 = 0.0350, wR_2 = 0.0854
Final R indexes [all data]	R_1 = 0.0476, wR_2 = 0.0919
Largest diff. peak/hole / e Å^{-3}	0.93/-0.87

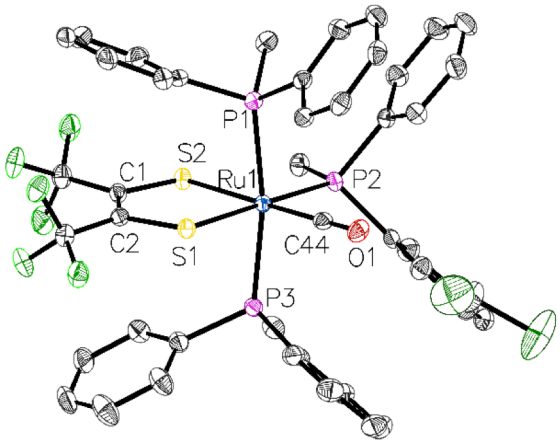

Table S9. Selected Crystallographic bond distances.

Bond	1[a]		2	3	4	5	6[b]	7	8	Average
	CO_{ap}	CO_{eq}	CO_{ap}	CO_{ap}	CO_{ap}	CO_{ap}	CO_{ap}	CO_{eq}	CO_{eq}	
C(1)–C(2)	1.350	1.359	1.355	1.359	1.362	1.356	1.342	1.354	1.349	1.354
C(1)–S(1)	1.735	1.718	1.740	1.727	1.732	1.733	1.763	1.728	1.725	1.733
C(2)–S(2)	1.726	1.717	1.735	1.737	1.737	1.738		1.732	1.745	1.733
C(5)–O(1)	1.149	1.135	1.158	1.158	1.214	1.167	1.150	1.148	1.152	1.159

Table S10. Selected DFT bonding parameters.

Bond	5			7	
	$CO_{equatorial}$	CO_{Axial}	CO_{TBP}	$CO_{equatorial}$	CO_{TBP}
C(1)–C(2)	1.38	1.38	1.37	1.38	1.37
C(1)–S(1)	1.74	1.74	1.76	1.73	1.75
C(2)–S(2)	1.73	1.74	1.76	1.74	1.76
C(5)–O(1)	1.20	1.20	1.19	1.19	1.19

Table S11. Location and peak areas for three-component Gaussian deconvolutions of the VT-FTIR for complex **4** in DCM.

Temperature (°C)	Location (cm^{-1})	Area
	1939.0	0.968
20	1968.0	1.050
	1975.3	0.216
	1938.8	0.989
10	1968.2	1.074
	1976.1	0.203
	1938.7	1.031
0	1968.6	1.038
	1977.1	0.192
	1938.6	1.080
–10	1968.6	1.089
	1977.3	0.182
	1938.5	1.139
–20	1968.9	1.120
	1977.3	0.174
	1938.4	1.210
–30	1969.0	1.116
	1977.7	0.167
	1938.3	1.276
–40	1969.3	1.071
	1978.0	0.150
	1938.2	1.381
–50	1970.1	1.051
	1978.2	0.104
	1938.2	1.490
–60	1970.6	0.923
	1979.0	0.113
	1938.1	1.551
–70	1970.8	1.040
	1980.0	0.055

Table S12. Location and peak areas for three-component Gaussian deconvolutions of the VT-FTIR for complex **5** in DCM.

Temperature (°C)	Location (cm^{-1})	Area
	1932.6	0.613
20	1967.5	1.000
	1975.4	0.063
	1932.5	0.637
10	1968.3	1.019
	1976.2	0.051
	1932.6	0.677
0	1968.8	1.009
	1976.6	0.050
	1932.1	0.693
–10	1969.4	1.017
	1977.0	0.040
	1931.9	0.703
–20	1969.9	1.046
	1977.5	0.034
	1931.8	0.713
–30	1970.2	1.050
	1978.0	0.029
	1937.1	0.728
–40	1970.3	1.069
	1978.2	0.026
	1931.5	0.726
–50	1970.5	1.082
	1978.7	0.023
	1931.2	0.740
–60	1970.8	1.106
	1979.6	0.019
	1931.2	0.770
–70	1970.9	1.143
	1980.1	0.015

Table S13. Location and peak areas for two-component Gaussian deconvolutions of the VT-FTIR for complex **7** in DCM.

Temperature (°C)	Location (cm^{-1})	Area
20	1956.2	3.77
	1974.2	0.41
10	1956.4	3.88
	1974.3	0.39
0	1956.9	3.99
	1974.7	0.38
–10	1957.1	4.03
	1974.9	0.38
–20	1957.6	4.16
	1975.3	0.36
–30	1958.2	4.28
	1975.8	0.34
–40	1958.8	4.43
	1976.2	0.31
–50	1959.2	4.42
	1976.6	0.30
–60	1959.9	4.56
	1977.0	0.27
–70	1960.6	4.71
	1977.6	0.24

Table S14. Location and peak areas for two-component Gaussian deconvolutions of the VT-FTIR for complex **8** in DCM.

Temperature (°C)	Location (cm^{-1})	Area
20	1952.0	0.591
	1968.3	1.198
10	1952.5	0.640
	1968.7	1.198
0	1952.7	0.669
	1968.9	1.184
–10	1953.4	0.697
	1969.5	1.175
–20	1953.6	0.729
	1969.6	1.173
–30	1953.8	0.761
	1969.8	1.158
–40	1954	0.790
	1969.9	1.145
–50	1954.1	0.830
	1970.0	1.118
–60	1954.2	0.841
	1970.1	1.123
–70	1954.3	.871
	1970.3	1.07

Table S15. Equilibrium constants for the isomerization of complex **4** using the peak areas from Table S11 as the population ratios to determine K_{eq}.

Temperature (°C)	K_{eq}: CO_{TBP}/CO_{eq}	K_{eq}: CO_{ax}/CO_{TBP}	K_{eq}: CO_{eq}/CO_{ax}
20	0.206	4.479	0.922
10	0.190	4.850	0.921
0	0.185	5.374	0.993
-10	0.167	5.943	0.991
-20	0.155	6.547	1.017
-30	0.149	7.255	1.085
-40	0.140	8.485	1.192
-50	0.099	13.246	1.314
-60	0.123	13.155	1.614
-70	0.053	28.410	1.497

Table S16. Equilibrium constants for the isomerization presented in complex **5** using the peak areas from Table S12 as the population ratios to determine K_{eq}.

Temperature (°C)	K_{eq}: CO_{TBP}/CO_{eq}	K_{eq}: CO_{ax}/CO_{TBP}	K_{eq}: CO_{eq}/CO_{ax}
20	0.063	9.739	0.613
10	0.051	12.407	0.631
0	0.049	13.671	0.668
-10	0.039	17.510	0.682
-20	0.033	20.504	0.672
-30	0.025	27.419	0.679
-40	0.024	28.347	0.680
-50	0.021	31.963	0.671
-60	0.018	38.036	0.669
-70	0.013	50.750	0.674

Table S17. Equilibrium constants for the isomerization of complexes **7** and **8** using the peak areas from Table S13 and S14 as the population ratios to determine K_{eq}.

Temperature (°C)	K_{eq}: CO_{eq}/CO_{TBP} (7)	K_{eq}: CO_{eq}/CO_{TBP} (8)
20	0.109	2.02
10	0.101	1.86
0	0.095	1.77
-10	0.092	1.69
-20	0.087	1.61
-30	0.079	1.52
-40	0.072	1.45
-50	0.068	1.35
-60	0.059	1.31
-70	0.051	1.23

Table S18. DFT optimized XYZ coordinates for the CO_{axial} isomer of complex **5**.

Atom	X	Y	Z
Ru	4.57142492	4.24036581	6.80652118
S	4.73353223	6.11731425	5.49878568
S	4.99284319	3.05590463	4.8704231
P	4.70689708	5.67467879	8.63189521
P	5.61619662	2.51269244	7.90759067
F	5.97690266	6.46001943	1.88538802
F	3.8321932	6.7397907	2.15607215
F	5.23992009	7.87411577	3.35751515
O	1.7618265	3.33362323	7.30124698
F	5.10506554	2.33558874	2.15617984
C	6.19074975	-1.3279468	6.45067632
H	7.01096143	-2.0548086	6.39916937
C	5.14827468	2.21956596	9.64925779
C	4.10826116	0.550794	6.57642502
H	3.29613463	1.28477682	6.59957256
C	4.06740598	7.3496321	8.26287081
C	6.40738917	-0.0785752	7.05472437
H	7.39532011	0.14179142	7.47393312
C	4.92989252	-1.6435275	5.91498007
H	4.76104386	-2.6184209	5.44178782
C	3.88879015	-0.7019632	5.98400268
H	2.90342261	-0.9355229	5.56328034
C	5.01328351	6.66180379	2.81221357
C	6.47727791	5.91494833	9.02651343
C	5.62207386	2.21206842	12.0438985
H	6.33659923	2.3382041	12.8662783
C	5.36850341	0.87135017	7.12595711
C	3.91341724	5.30189787	10.257782
H	4.36545431	4.36802077	10.6274764
H	4.21008369	6.12032071	10.940128
C	6.05951525	2.35918251	10.715316
H	7.11014187	2.60235547	10.5255999
C	3.80102655	1.90073628	9.92978807
H	3.08032917	1.80056333	9.11006699
C	4.76848883	8.51479687	8.62817277
H	5.73471198	8.43587075	9.14059833
C	2.39336328	5.17440574	10.1844229

H	2.08318147	4.37175095	9.49792868
H	1.92139998	6.11378658	9.84756643
H	1.99193811	4.93622631	11.1847634
C	4.99954055	5.5728171	3.86412955
C	7.33617316	6.30007698	7.97132242
H	6.90430922	6.51325727	6.98476945
C	4.2778849	1.90780917	12.3160593
H	3.93768211	1.79697494	13.3527974
C	7.02495578	5.62263978	10.2919303
H	6.37954773	5.32827681	11.1255223
C	5.08632094	4.22557348	3.59037751
C	2.83044572	7.46461975	7.59170262
H	2.29642592	6.55993103	7.27907403
C	2.29519913	8.73024794	7.30947029
H	1.33206602	8.80940835	6.79168672
C	4.23749175	9.78171356	8.33315378
H	4.79351208	10.6836257	8.61651806
F	4.60345724	4.2484397	1.26138159
C	3.00008563	9.89099078	7.67481655
H	2.58783205	10.8802001	7.44089055
C	8.71981223	6.37994066	8.1772351
H	9.37519973	6.67805051	7.35021687
C	9.26516422	6.05771654	9.43506091
H	10.3501322	6.10026513	9.59182565
F	6.65724453	3.82141517	1.85789337
C	3.36921473	1.74114913	11.2537998
H	2.31955095	1.49849675	11.4575059
C	7.44231512	2.78170374	7.93687895
H	7.60498261	3.62562653	8.62963913
H	7.92691575	1.89530654	8.38498919
C	8.41576518	5.68569591	10.4908466
H	8.83401261	5.44034133	11.4746882
C	8.01349858	3.11053679	6.55710091
H	7.7668375	2.33265936	5.81325315
H	9.11083286	3.21282923	6.61718875
H	7.59506245	4.05893941	6.1801872
C	5.36201416	3.657493	2.21102657
C	2.90153688	3.68914376	7.18048218

Table S19. DFT optimized XYZ coordinates for the $CO_{equatorial}$ isomer of complex **5**.

Atom	X	Y	Z
Ru	4.59381182	4.35349639	7.03125611
S	4.03000066	6.09059398	5.59872012
S	6.15608883	3.79273173	5.44601229
P	5.02393104	5.84591419	8.65780201
P	5.45283567	2.5429265	8.21060297
F	6.19841812	7.693729	2.95473504
F	4.49586093	6.64271861	2.08426246
F	4.18734506	8.09906314	3.661791
O	1.72667376	3.86060313	7.86429939
F	7.81799958	3.77501037	3.15969379
C	6.45025187	-1.1714866	6.64817683
H	7.17218405	-1.9703146	6.85924252
C	4.46828564	1.96540955	9.64747617
C	4.61577127	0.88675754	6.10910642
H	3.91911554	1.70459734	5.88643576
C	4.09541664	7.41862118	8.5248042
C	6.44572429	-0.0101933	7.43868472
H	7.158458	0.07388109	8.26807838
C	5.53165365	-1.3087357	5.59172819
H	5.53510221	-2.216373	4.97536902
C	4.61112703	-0.2792526	5.32699816
H	3.89350542	-0.3782286	4.50312173
C	5.00768001	7.11758895	3.24050495
C	6.78046161	6.29965978	8.43826655
C	4.12075144	1.62595895	12.0419829
H	4.50348411	1.68201748	13.06853
C	5.52876225	1.0271852	7.17531508
C	4.81378848	5.40397344	10.4335991
H	5.46269262	4.53400474	10.632596
H	5.19951791	6.25760825	11.0228838
C	4.94563256	2.01639393	10.9726569
H	5.96163586	2.36297985	11.1905071
C	3.16637302	1.47524459	9.40671944
H	2.78881843	1.40764648	8.3806022
C	4.73997534	8.65017261	8.7545187
H	5.80688711	8.67161883	9.00732788
C	3.36432799	5.08564839	10.7985743

H	2.97053845	4.25003692	10.1989296
H	2.70852805	5.95963511	10.6435018
H	3.30212661	4.79388467	11.8604764
C	5.15688935	6.02372089	4.28197212
C	7.18873279	6.68875228	7.14183597
H	6.43835176	6.7849038	6.34902655
C	2.81719232	1.16469342	11.7962241
H	2.17238773	0.86393192	12.6305829
C	7.74243712	6.17100803	9.45920201
H	7.44819166	5.88421137	10.4749988
C	6.10289782	5.02331182	4.2146318
C	2.72524995	7.40432154	8.1895585
H	2.21694269	6.45376135	7.99588393
C	2.00910702	8.60663382	8.09641357
H	0.94498663	8.58384109	7.83282407
C	4.02276766	9.85417822	8.65391041
H	4.53521802	10.8079964	8.82975374
F	6.8249952	5.28499014	1.95849517
C	2.65689945	9.83463617	8.32309485
H	2.09819317	10.7748008	8.23755476
C	8.54149049	6.91321846	6.86388282
H	8.84147642	7.17879073	5.84412141
C	9.50362673	6.761884	7.88086113
H	10.5660149	6.92295518	7.66022809
F	8.20727264	5.87823668	3.53586823
C	2.34564553	1.08151395	10.4730302
H	1.3345336	0.70986873	10.2693635
C	7.15933002	2.74203107	8.89577428
H	7.08829025	3.56800296	9.62602033
H	7.41240487	1.83087847	9.4692819
C	9.1015124	6.40095428	9.17774846
H	9.84572857	6.28802889	9.97535638
C	8.23040843	3.06742914	7.85611588
H	8.3230398	2.26651993	7.10185295
H	9.20742248	3.19351207	8.35332568
H	7.9934302	3.99789433	7.31718074
C	7.23355859	4.98747644	3.21124647
C	2.87289082	4.07958426	7.60345835

Table S20. DFT optimized XYZ coordinates for the CO_{TBP} isomer of complex **5**.

Atom	X	Y	Z
Ru	3.96980197	4.33102779	6.6696818
S	4.72788646	5.67179706	4.97221931
S	6.16265685	3.42511312	6.88768247
P	4.63314841	5.88381938	8.28148137
P	3.42210149	2.50142422	5.38483733
F	8.39939523	6.31167397	4.01252812
F	7.13425536	5.26854729	2.57544286
F	6.48140502	7.15011342	3.44362009
O	1.14203045	5.44139224	6.42460142
F	8.6896522	2.64674062	6.02542824
C	0.15654754	1.68915148	2.98436048
H	-0.5377892	0.86139561	2.79351404
C	2.81587216	1.79697473	6.9555507
C	1.93450697	3.81854166	3.47763203
H	2.6481168	4.63027839	3.6757436
C	3.63043716	7.41103966	8.37973118
C	1.17883296	1.53836209	3.93492314
H	1.28366117	0.59292804	4.48266087
C	0.02628154	2.89951122	2.27738034
H	-0.7729712	3.01519205	1.5344766
C	0.9187796	3.9595347	2.51907732
H	0.82137752	4.90069411	1.96419929
C	7.12084782	5.98984104	3.72681182
C	6.33603042	6.50005569	8.0687795
C	3.3537257	1.02111627	9.2183674
H	4.09904143	0.69524346	9.95317324
C	2.06533203	2.60598726	4.18883812
C	4.54814179	5.0852264	9.93911583
H	5.26691455	4.24678376	9.87874786
H	4.89662447	5.77365523	10.7306317
C	3.76830083	1.37284137	7.92312924
H	4.8320395	1.33603567	7.6590004
C	1.4506361	1.8939457	7.33093424
H	0.71271455	2.2584271	6.6068514
C	3.32350955	8.03593509	9.60566352
H	3.68783435	7.61547984	10.5502094
C	3.13352968	4.55290059	10.190654

H	2.83517191	3.84352331	9.39746202
H	2.38544965	5.36541675	10.2056541
H	3.08066926	4.02006486	11.1559596
C	6.43419762	5.25220441	4.84801652
C	6.59107348	7.49804202	7.1031406
H	5.76219357	7.93327523	6.53678824
C	1.99634621	1.09972423	9.57059163
H	1.67460429	0.82920188	10.5830973
C	7.4188578	5.91901465	8.76106872
H	7.24568425	5.12845326	9.49868993
C	7.01776273	4.27020532	5.60646421
C	3.16072398	7.98252873	7.17670335
H	3.4094207	7.49966732	6.22380036
C	2.40511198	9.1644814	7.20140463
H	2.05367002	9.60201233	6.25921487
C	2.55435113	9.21153482	9.62941711
H	2.31680213	9.68574512	10.5894412
F	8.78226934	3.68813006	4.12444752
C	2.09511598	9.77911042	8.42766901
H	1.49959716	10.6999988	8.44711693
C	7.90663534	7.90276137	6.83176372
H	8.09139746	8.66281344	6.0631234
C	8.97952103	7.32253105	7.52723362
H	10.0087184	7.63171562	7.3079587
F	9.3440073	4.71165009	5.96434882
C	1.04893367	1.54325816	8.62622749
H	-0.0092534	1.62078787	8.90389336
C	4.69772636	1.4141673	4.63964322
H	5.49387924	1.34624155	5.4033277
H	4.26504336	0.41390801	4.4573344
C	8.73271293	6.33273587	8.49311875
H	9.56705156	5.86703319	9.03092718
C	5.24997609	2.06602267	3.36587525
H	4.46132818	2.21242799	2.60645838
H	6.03281272	1.42475959	2.92381367
H	5.70420623	3.04625786	3.58488121
C	8.45650991	3.83925902	5.43256791
C	2.24993123	5.02168711	6.52622512

Table S21. DFT optimized XYZ coordinates for the CO_{axial} isomer of complex **7**.

Atom	X	Y	Z
Ru	4.44923757	4.19404094	7.04063475
S	5.8510056	5.65502076	5.91767431
S	3.74621585	3.64392047	4.93412174
P	4.61301588	5.7995343	8.81247144
P	5.71056338	2.42465404	7.77300394
F	7.21583047	5.40777341	2.43912536
F	5.89447785	7.1009945	2.67004411
F	7.5248129	6.8125393	4.03136438
O	1.99406189	2.76437554	8.03885078
F	3.39900811	3.4391696	2.16535137
C	5.16604578	-1.6455469	7.52295926
H	5.50452111	-2.5099754	8.0820754
C	5.73197718	2.09700377	9.57487671
C	4.31035229	0.57953635	6.12497998
H	3.97281173	1.43501223	5.55830067
C	4.12063413	7.42535479	8.12062492
C	5.54820391	-0.3796923	7.92991548
H	6.16953464	-0.2815527	8.80984309
C	4.34971613	-1.8064818	6.4124047
H	4.04350929	-2.7973283	6.09784685
C	3.92470422	-0.6889515	5.71645552
H	3.28450414	-0.7937773	4.84835621
C	6.57939458	6.16551306	3.34101619
C	6.2857653	6.14263566	9.46503853
C	6.72385196	2.12038208	11.7779306
H	7.56016108	2.37817933	12.4179394
C	5.12705255	0.75912937	7.23417068
C	3.43535027	5.7246156	10.2906476
C	6.7826144	2.42458773	10.4242619
H	7.66339677	2.91696407	10.0427324
C	4.61338321	1.46222895	10.1224136
H	3.78233409	1.19041178	9.48315815
C	4.58167088	8.62949071	8.64723683
H	5.31559482	8.62804747	9.44334975
C	2.02240225	5.96186153	9.75537855
H	1.77411116	5.29714384	8.92739135
H	1.87901144	6.99008215	9.42512863

H	1.31225396	5.75942355	10.562265
C	5.68274161	5.34650294	4.24360495
C	7.17292261	6.90130942	8.69613173
H	6.84548122	7.33502659	7.76097095
C	5.61326552	1.48354183	12.3052023
H	5.57136589	1.24030251	13.3603675
C	6.75062195	5.60419756	10.6630695
H	6.10032345	5.01052547	11.2865337
C	4.76562357	4.44038624	3.80844114
C	3.18715517	7.46291865	7.08720716
H	2.83049359	6.5364933	6.65126747
C	2.72152202	8.67017336	6.59672441
H	1.99826348	8.67718304	5.7897319
C	4.12611442	9.83989393	8.14724026
H	4.50657285	10.7665457	8.56077531
F	4.71847119	4.98788337	1.49313565
C	3.19242859	9.86361356	7.12351629
H	2.83874289	10.8092089	6.72988059
C	8.47712238	7.1074221	9.11280914
H	9.14521448	7.69626207	8.49521357
C	8.92519134	6.56663928	10.3085569
H	9.94467808	6.73228547	10.6361295
F	5.51305655	3.06276744	2.05273915
C	4.55466236	1.15575664	11.4687668
H	3.67703341	0.66008414	11.8670297
C	7.48867208	2.42157102	7.14331613
C	8.05498361	5.81690085	11.082643
H	8.38706318	5.3946504	12.0241336
C	7.3892741	2.31726223	5.62088712
H	6.92334153	1.38103749	5.30986051
H	8.39862399	2.34590585	5.20117006
H	6.82487936	3.1429007	5.18981478
C	4.59781243	3.99281755	2.37552173
C	2.94881687	3.31094407	7.71001506
C	8.28372154	1.22216388	7.65576312
H	7.87630094	0.27956627	7.29283588
H	8.34491086	1.17990231	8.74365674
H	9.3034519	1.30826056	7.27023373
C	3.74271254	6.80940441	11.3179915
H	3.68940005	7.80637609	10.880286

H	4.71958943	6.69097815	11.7868722
H	2.98678025	6.75735237	12.1081412
C	3.46274379	4.35129193	10.9460202
H	3.07849301	3.58777662	10.2742104
H	2.81508235	4.36937085	11.8276224
H	4.4514596	4.03269624	11.2707117
C	8.22332326	3.70853797	7.50434539
H	7.73808799	4.58078708	7.07267019
H	9.23312019	3.6511421	7.08863131
H	8.32123376	3.87716912	8.57566026

Table S22. DFT optimized XYZ coordinates for the $CO_{equatorial}$ isomer of complex **7**.

Atom	X	Y	Z
Ru	4.67971752	8.17199316	10.097693
S	5.58430583	10.272366	9.95097883
S	5.77042708	8.0421056	12.143588
P	4.87627754	5.88370779	9.64137026
P	2.62129794	8.27937666	11.0565
F	8.06140925	12.0501951	12.3461465
F	6.01844578	12.7969632	12.1852914
F	7.23076315	12.5375476	10.403418
F	6.65304453	8.87061657	14.676941
F	6.6530203	11.0141546	14.3363221
F	8.38738702	9.81224404	13.7789742
O	3.82885862	8.61767448	7.21004579
C	6.42096342	10.5753081	11.4463915
C	6.94128847	11.9872814	11.5994474
C	6.43299909	9.61387635	12.4349201
C	7.03604164	9.82801025	13.8112438
C	3.48606083	5.30498636	8.59532227
C	2.35143215	4.73965258	9.2192201
H	2.36660942	4.53507325	10.2931308
C	1.19785361	4.43738276	8.48081404
H	0.32928855	4.00488976	8.99277422
C	1.15552589	4.69293444	7.09955504
H	0.25224441	4.46298204	6.52126432
C	2.28331107	5.24088308	6.46459644
H	2.26830458	5.44012538	5.38610897
C	3.43996647	5.53821364	7.20323088
H	4.29809594	5.96960971	6.68294655
C	6.52736071	5.68215753	8.68129691
C	6.5601979	4.32496265	7.96270276
H	5.78626357	4.24282024	7.18089304
H	6.42405738	3.48917107	8.67063283
H	7.54580271	4.19568872	7.47691396
C	7.65648489	5.76405155	9.72674991
H	7.67905753	4.88371905	10.3898058
H	7.56125716	6.6715954	10.3515676
H	8.62601049	5.81513794	9.19731968
C	6.73098238	6.84714717	7.69372831

H	7.68937964	6.69306063	7.16336509
H	6.78896325	7.81181583	8.22887084
H	5.93993738	6.93804605	6.93293261
C	5.05240288	4.54731027	10.8967174
C	5.72274311	4.80544938	12.1114057
H	6.06994033	5.81865276	12.3298214
C	5.93639086	3.78533765	13.0492094
H	6.45571922	4.01733866	13.9868183
C	5.47700181	2.48192053	12.7929889
H	5.63260865	1.68505209	13.5307729
C	4.8219756	2.20703402	11.5806278
H	4.46761176	1.1925132	11.3610873
C	4.62183091	3.22765384	10.637079
H	4.11875386	2.98562677	9.69487947
C	4.10050324	8.40104969	8.3515035
C	2.69821396	9.36224301	12.5490077
C	3.39676593	10.5854921	12.4943138
H	3.8907353	10.8772124	11.5623281
C	3.49798193	11.4063903	13.626726
H	4.08153157	12.3297616	13.5630897
C	2.8968345	11.0165677	14.8349853
H	2.99060384	11.6479048	15.7273974
C	2.18022954	9.80892631	14.895449
H	1.7002141	9.49802849	15.8315361
C	2.08195727	8.98552005	13.7620006
H	1.52469265	8.04572199	13.8294019
C	1.25558607	9.07211316	10.0107589
C	0.03184463	9.37723599	10.9006572
H	-0.7709645	9.79703872	10.2660045
H	0.28027846	10.1251898	11.6720355
H	-0.374698	8.49072599	11.4117686
C	1.79179391	10.4111611	9.4662688
H	2.66683788	10.2810988	8.81349732
H	2.06406102	11.1043835	10.2788442
H	0.99126821	10.8893614	8.8713212
C	0.90052968	8.14159972	8.83602203
H	0.48986935	7.17276419	9.15256312
H	1.77249836	7.9338266	8.19888374
H	0.14147855	8.64102296	8.20455168
C	1.98560141	6.71601105	11.7845644

C	2.88601668	6.05939093	12.6531273
H	3.86100474	6.52148931	12.8468946
C	2.54842939	4.84226023	13.2576027
H	3.27550404	4.34402877	13.9086981
C	1.29714768	4.25381646	13.0033323
H	1.03736366	3.29073789	13.458313
C	0.38126531	4.91002607	12.1644058
H	-0.6014851	4.46675223	11.964219
C	0.72119411	6.13302594	11.5619985
H	-0.0113934	6.60597398	10.9057657

Table S23. DFT optimized XYZ coordinates for the CO_{TBP} isomer of complex **7**.

Atom	X	Y	Z
Ru	4.87617465	8.43521056	9.95123136
S	5.66063282	10.5609437	10.3648476
S	5.56105731	7.85096429	12.179417
P	6.93566108	7.66628005	9.09185474
P	2.71753479	8.56561067	10.8953229
F	8.17264009	11.587246	13.1091642
F	6.19375124	12.505706	13.1080195
F	7.39687679	12.4986657	11.3005149
F	6.41113416	8.19366778	14.8156614
F	6.62649978	10.3509806	14.8577028
F	8.25294475	9.10210391	14.1129979
O	3.97388925	9.26692633	7.16229748
C	6.43682375	10.4413347	11.943639
C	7.05278472	11.7478542	12.3738561
C	6.31985658	9.32343459	12.7336588
C	6.89725921	9.24413085	14.1281989
C	5.92171601	6.34861127	8.31717626
C	5.10948348	5.64600353	9.26399056
H	5.37633365	5.6665073	10.3302194
C	3.99155023	4.909157	8.83427511
H	3.36600401	4.39952806	9.5753998
C	3.68696169	4.83258041	7.46623598
H	2.8116965	4.26476287	7.12855773
C	4.51158746	5.48020547	6.52588973
H	4.28384715	5.40577205	5.45535695
C	5.61262263	6.24328605	6.94379256
H	6.21370443	6.77241186	6.19727331
C	8.0192979	8.63031112	7.90362648
C	8.95774853	7.68538158	7.13718438
H	8.40706881	6.99063974	6.47910418
H	9.5785046	7.0853778	7.82593706
H	9.63887275	8.28306576	6.5014359
C	8.81803782	9.59516376	8.80798365
H	9.52053091	9.06030401	9.46904394
H	8.13490249	10.207863	9.42509674
H	9.40945791	10.2740735	8.16484797
C	7.14353906	9.4685182	6.95894217

H	7.80596612	10.0353368	6.27778663
H	6.54251371	10.1952275	7.52898635
H	6.45905217	8.86686167	6.34107331
C	8.08584505	6.78240696	10.1912954
C	8.574914	7.4294765	11.3463983
H	8.28068176	8.46130757	11.5621276
C	9.43574922	6.75309021	12.2231945
H	9.790725	7.263696	13.1250269
C	9.80635403	5.42189184	11.9624503
H	10.4723173	4.89173989	12.6549687
C	9.31519472	4.76763665	10.8186807
H	9.60078154	3.72983731	10.6090305
C	8.45251415	5.44423138	9.93944852
H	8.06481586	4.92734289	9.05326892
C	4.31729392	8.93517277	8.25411141
C	2.65888977	9.26048363	12.5900387
C	3.38700187	10.4399152	12.8521814
H	3.96823139	10.8965441	12.0430557
C	3.40863831	10.9915288	14.140494
H	4.01907709	11.8808867	14.3273932
C	2.69168011	10.3772032	15.1816687
H	2.71893005	10.7993828	16.1940738
C	1.94351261	9.21472341	14.9227612
H	1.37812106	8.73206096	15.7296023
C	1.92683437	8.65753558	13.6333611
H	1.35192829	7.74333966	13.4473618
C	1.39389617	9.52103845	9.94335184
C	0.08828405	9.59725685	10.7562112
H	-0.6737214	10.1488107	10.1740508
H	0.23954459	10.1307442	11.7101176
H	-0.3183783	8.59733196	10.987029
C	1.96807829	10.9415595	9.7622221
H	2.91797276	10.9334537	9.20437599
H	2.14676131	11.4369814	10.7313491
H	1.23964105	11.5531846	9.19787902
C	1.16849642	8.85597035	8.55652295
H	0.16956839	8.39227919	8.49468273
H	1.91285222	8.07761811	8.32156789
H	1.23567568	9.60920412	7.75395399
C	2.13592996	6.83060851	11.1226544

C	2.87059758	6.02269082	12.0251999
H	3.71243547	6.47009175	12.5683125
C	2.54176312	4.67416459	12.2174613
H	3.1282439	4.07150644	12.9218337
C	1.46757392	4.09972319	11.5119347
H	1.20779227	3.04469619	11.6610769
C	0.7287087	4.89193165	10.6182206
H	-0.1143394	4.46018506	10.065303
C	1.05835379	6.24562253	10.425849
H	0.46084693	6.83034179	9.72388526

References.

1. Balch, A. L.; Miller, J., 1,2-Dithiolene complexes of ruthenium and iron. *Inorg. Chem.* **1971,** *10* (7), 1410-1415.
2. Porter, Tyler M.; Wang, J.; Li, Y.; Xiang, B.; Salsman, C.; Miller, J. S.; Xiong, W.; Kubiak, C. P., Direct observation of the intermediate in an ultrafast isomerization. *Chemical Science* **2019,** *10* (1), 113-117.
3. Neese, F., An improvement of the resolution of the identity approximation for the formation of the Coulomb matrix. *J. Comput. Chem.* **2003,** *24* (14), 1740–1747.
4. Kossmann, S.; Neese, F., Comparison of two efficient approximate Hartee–Fock approaches. *Chem. Phys. Lett.* **2009,** *481* (4–6), 240–243.
5. Neese, F.; Wennmohs, F.; Hansen, A.; Becker, U., Efficient, approximate and parallel Hartree–Fock and hybrid DFT calculations. A 'chain-of-spheres' algorithm for the Hartree–Fock exchange. *Chem. Phys.* **2009,** *356* (1–3), 98–109.
6. Izsák, R.; Neese, F., An overlap fitted chain of spheres exchange method. *J. Chem. Phys.* **2011,** *135* (14), 144105.
7. Neese, F., The ORCA program system. *Wiley Interdisciplinary Reviews: Computational Molecular Science* **2012,** *2* (1), 73–78.
8. Huzinaga, S.; Andzelm, J.; Radzio-Andzelm, E.; Sakai, Y.; Tatewaki, H.; Klobukiwski, M., *Gaussian Basis Sets for Molecular Calculations*. Elsevier Science: 1983; Vol. 16, p 434.
9. Andrae, D.; Häußermann, U.; Dolg, M.; Stoll, H.; Preuß, H., Energy-adjustedab initio pseudopotentials for the second and third row transition elements. *Theor. Chem. Acc.* **1990,** *77* (2), 123–141.
10. Schäfer, A.; Horn, H.; Ahlrichs, R., Fully optimized contracted Gaussian basis sets for atoms Li to Kr. *J. Chem. Phys.* **1992,** *97* (4), 2571–2577.
11. Schäfer, A.; Huber, C.; Ahlrichs, R., Fully optimized contracted Gaussian basis sets of triple zeta valence quality for atoms Li to Kr. *J. Chem. Phys.* **1994,** *100* (8), 5829–5835.
12. Weigend, F., Accurate Coulomb-fitting basis sets for H to Rn. *Phys. Chem. Chem. Phys.* **2006,** *8* (9), 1057–1065.
13. Pantazis, D. A.; Neese, F., All-electron scalar relativistic basis sets for the 6p elements. *Theor. Chem. Acc.* **2012,** *131* (11), 1292.
14. Pantazis, D. A.; Neese, F., All-Electron Scalar Relativistic Basis Sets for the Actinides. *J. Chem. Theory Comput.* **2011,** *7* (3), 677-684.
15. Pantazis, D. A.; Neese, F., All-Electron Scalar Relativistic Basis Sets for the Lanthanides. *J. Chem. Theory Comput.* **2009,** *5* (9), 2229-2238.
16. Pantazis, D. A.; Chen, X.-Y.; Landis, C. R.; Neese, F., All-Electron Scalar Relativistic Basis Sets for Third-Row Transition Metal Atoms. *J. Chem. Theory Comput.* **2008,** *4* (6), 908-919.
17. Sinnecker, S.; Rajendran, A.; Klamt, A.; Diedenhofen, M.; Neese, F., Calculation of Solvent Shifts on Electronic g-Tensors with the Conductor-Like Screening Model (COSMO) and Its Self-Consistent Generalization to Real Solvents (Direct COSMO-RS). *J. Phys. Chem. A* **2006,** *110* (6), 2235–2245.
18. Grimme, S.; Ehrlich, S.; Goerigk, L., Effect of the damping function in dispersion corrected density functional theory. *J. Comput. Chem.* **2011,** *32* (7), 1456–1465.

19. Grimme, S.; Antony, J.; Ehrlich, S.; Krieg, H., A consistent and accurate ab initio parametrization of density functional dispersion correction (DFT-D) for the 94 elements H-Pu. *J. Chem. Phys.* **2010,** *132* (15), 154104.
20. Pettersen, E. F.; Goddard, T. D.; Huang, C. C.; Couch, G. S.; Greenblatt, D. M.; Meng, E. C.; Ferrin, T. E., UCSF Chimera–a visualization system for exploratory research and analysis. *J. Comput. Chem.* **2004,** *25* (13), 1605–1612.